# Supporting information

## Covalent Heterojunction Enhances Electron Transfer and Oxygen Activation for Photocatalytic C($sp^3$)−C($sp^2$) Cross-Dehydrogenative Coupling Reaction

Jincong Yuan, [a] Lingjuan Zhang,[a] Xian-Ming Zhang*[a, b]
E-mail: mail: zhangxm@dns.sxnu.edu.cn

# Table of Contents

# Section S1. Instrument and Methods

All the chemicals were purchased from commercial sources and used without further purification, unless otherwise stated. PXRD patterns were measured on Rigaku D/Max-2500 diffractometer with Cu target tube at 40 kV and 30 mA. X-ray photoelectron spectroscopy (XPS) was carried out on a Thermo Fisher SCIENTIFIC using Al Kα X-ray source. Binding energies (BE) were calibrated by setting the measured BE of C1s to 284.8 eV. Thermogravimetric analyses (TGA) were performed on Shanghai yinnuo 1000 B under $N_2$ atmosphere at a heating rate of 10°C $min^{-1}$. Nuclear magnetic resonance (NMR) data were recorded on Bruker Avance III DM 600 MHz. $N_2$ adsorption-desorption isotherms were measured using a Micrometritics ASAP 2420 system at 77 K. Mass spectra were achieved on Q EXACTIVE (thermo). UV-vis spectra were tested on a LAMBDA650 spectrophotometer and $BaSO_4$ was used as the reflectance standard reference. The morphology analysis of the as-prepared samples was conducted on a scanning electron microscope (SEM, S4800, Hitachi Co., Japan). Samples for SEM tests were dispersed in EtOH with the aid of sonication, and then deposited on a conductive tape. Transmission electron microscopy (TEM) investigations was performed by JE0L-JEM F200. Prior to TEM measurements, samples were dispersed in ethanol using a sonication method, and then mounted on a carbon coated molybdenum grid. The PL spectra of samples and the PL lifetime were recorded on the powder samples by using Edinburgh FLS920 fluorescence spectrometer with a picosecond pulsed diode laser. Electron paramagnetic resonance (EPR) measurements were carried out on a Bruker model A300 spectrometer.

Characterization of products all products were isolated by flash column chromatography on silica gel with petroleum ether/ethyl acetate as eluent. Products are known compounds and are characterized by comparison of their $^1H$ NMR, $^{13}C$ NMR spectroscopic data and mass data with those reported in the literature. All chemical shifts ($\delta$) are reported in ppm and coupling constants ($J$) in Hz. All chemical shifts were reported relative to tetramethylsilane (0 ppm for $^1H$) and $CDCl_3$ (77.16 ppm for $^{13}C$), respectively.

## 1. Electrochemical measurements

The polymer (5 mg) was well dispersed in 0.2 mL ethanol containing 10 $\mu$L nafion and sonicated for 30 min. Next, the suspension was dispersed dropwise onto the surface of a clear ITO glass with exposed 1×1 $cm^2$ area, drying overnight in oven. The photo-electrochemical measurements were carried out in CHI-660 electrochemical station (Chenhua instrument, Shanghai, China). The as-synthesized photoanode of the polymer was used as working electrode in a common three electrode configuration with Pt foil as the counter electrode and Ag/AgCl (saturated KCl) as the reference electrode. $Na_2SO_4$ (0.2 M) solution was used as the electrolyte and Xe lamp (300W, CEL-HXE 300, Beijing China Education Au-light Technology Co., Ltd.) was used as the light source. The photocurrent response was measured at +0.4 V bias voltage under chopped light. The Mott Schottky measurement in the dark was carried out at frequency of 300/500/1000 Hz. The electrochemical impedance spectra were obtained by immersing in the frequency range from $10^{-2}$ to $10^6$ Hz with a bias potential of 0.4 V.

## 2. Synthesis method of photocatalysts

### 2.1 Ligand Synthesis: referring to literature, the ligands were successfully synthesized.[1,2]

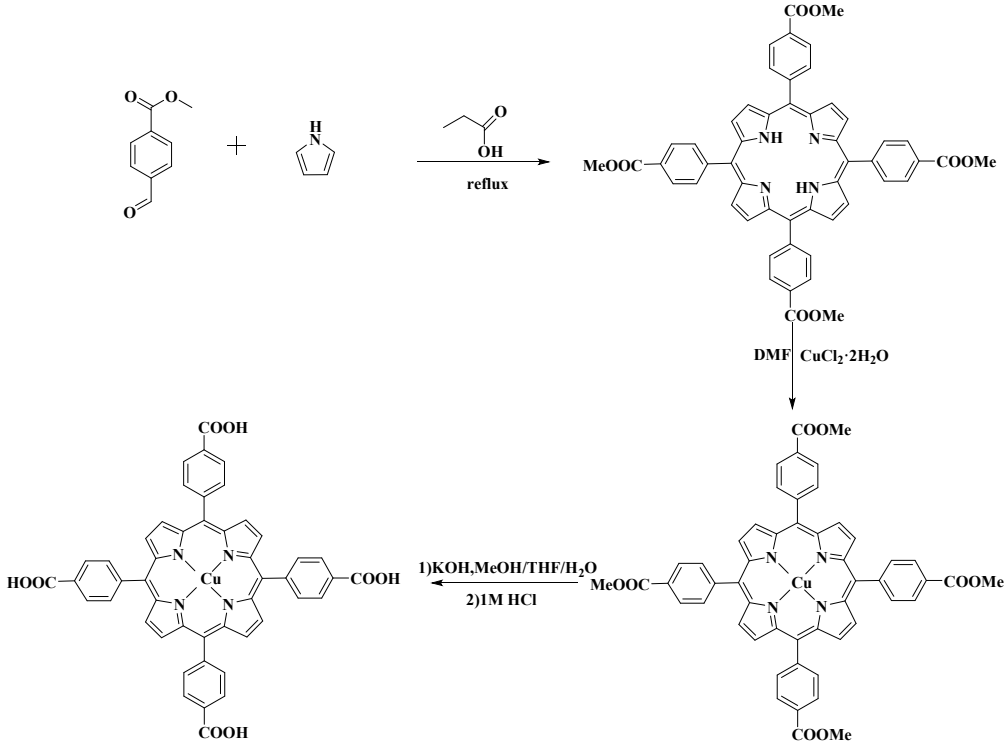

**2.2 Synthesis of PCN-222(Cu)[2]**

$ZrOCl_2 \cdot 8H_2O$ (50 mg) and benzoic acid (750 mg) in 5 mL of DMF were ultrasonically dissolved for 30 min. The mixture was heated in 80°C oven for one hour. After cooling to room temperature, CuTCPP (25 mg) was added and ultrasonically dissolved for 10 minutes. The mixture was heated at 120°C in an oil bath for 1 hour. After cooling down to room temperature, red powder was obtained by filtrating, washing with DMF and ethanol, and drying in a vacuum oven at 80°C.

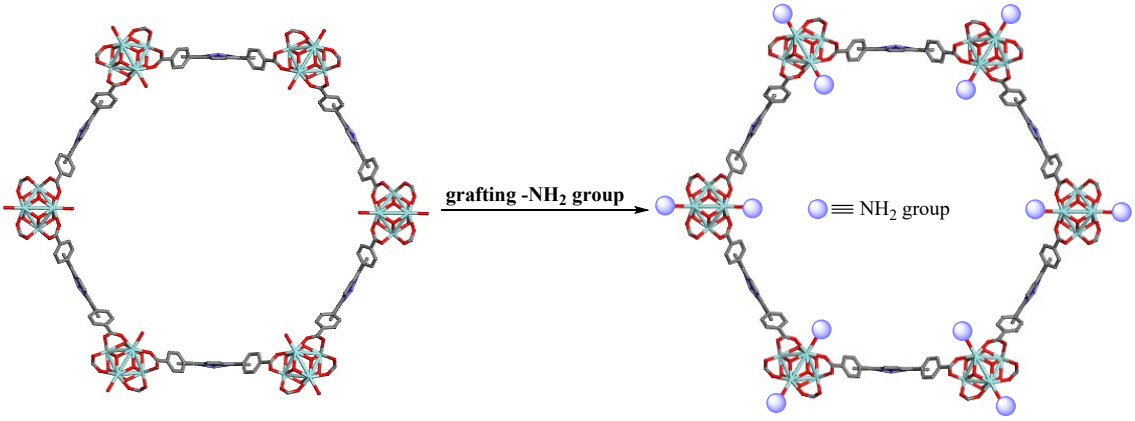


**2.3 Synthesis of PCN-222(Cu)-$NH_2$[3]**

Typically, 80 mg activated PCN-222(Cu), 4-aminobenzoic acid (ABA, 4 mmol), and 10 mL dry DMF were mixed, and the mixture was stirred in an oil bath at 60 °C for 24 hours. After cooling down to room temperature, the obtained PCN-222(Cu)-$NH_2$ were washed with DMF, acetone, and methanol for at least 3 times respectively by centrifugation, and further soaked in acetone for 3 days to remove free 4-aminobenzoic acid in the MOF pores. The final sample was obtained after finally drying under vacuum at 80 °C.

**2.4 Synthesis of TR-1[4]:**

1,3,5-tri-(4-aminophenyl) triazine (TTA, 0.10 mmol, 35.4 mg) and terephthaldehyde (TPA 0.15 mmol, 20.12 mg) in the presence of acetic acid (6 M, 0.6 mL) were mixed in o-DCB/n-BuOH (3/3 mL) under ultrasonication for 15 min. Then, acetic acid (6 M, 0.6 mL) was added to the mixed solution in the Teflon-lined autoclave (25 mL). The autoclave was sealed and heated at 120 °C for 3 days. The residue was washed with DMF, $H_2O$, THF, and $CH_3OH$ to remove the

unreacted molecules. Afterward, the crude product was further washed by Soxhlet extraction with $CH_3OH$ as solvents until the filtrate became colorless. The solid was dried at 80 °C in a vacuum to produce TR-1 powder with 70% isolated yield.

**2.5 Synthesis of PCN-222(Cu)TR-1[5]:**

First, the PCN-222(Cu)-$NH_2$ (25 mg), TPA (0.15 mmol, 20.12 mg), and o-DCB/n-BuOH (3/3 mL) were mixture in a 25 mL Teflon-lined autoclave and sonicated 1 h at room temperature to uniformly distribute the TPA on the PCN-222(Cu)-$NH_2$ surface. Afterward, TTA (0.1 mmol, 35.4 mg) and 1.2 mL acetic acid aqueous solution (6 M) were added and continued to sonicate for 30 min to get a homogenous dispersion. The autoclave was sealed and heated at 120 °C for 3 days. The residue was washed with DMF, $H_2O$, THF, and $CH_3OH$ to remove the unreacted molecules. Then, the crude product was further washed by Soxhlet extraction with $CH_3OH$ as solvents until the filtrate became colorless. The solid was dried at 80 °C in a vacuum to produce PCN-222(Cu)TR-1 powder with 85% isolated yield. The weight loading of Cu was determined to be 1.04 % using an inductively coupled plasma-atomic emission spectrometry (ICP-OES).

**3. A general procedure for aerobic photocatalytic C($sp^3$)-C($sp^2$) cross-dehydrogenative coupling reaction**

In a typical experiment, PCN-222(Cu)@TR-1 (10 mg) was added in a mixture of $CH_3CN$ (2 mL), phenyl glycinate (**1a**, 0.1 mmol) and indole (**2a**, 0.13 mmol) under $O_2$ atmosphere. In a 5 mL branched Schlenk tube with gentle stirring, the reaction was irradiated with a 300 W Xe Lamp and monitored by TLC. Followed by phenyl glycinate (**1a**) was exhausted completely, the reaction was cooled down to room temperature and quenched in (10 mL) saturated NaCl solution then extracted with EtOAc (3 × 10 mL). After the reaction, the catalyst was separated by centrifugation, thoroughly washed with methanol, and then reused in subsequent runs. The combined organic layers was concentrated in vacuo, then the residue was purified by flash column chromatography (petroleum ether: ethyl acetate = 4 : 1) to get product **3a**.

**4. Recycle test**

After the first run catalysis was completed, the photocatalyst PCN-222(Cu)@TR-1 was recycled by centrifugation then washed with water and methanol repeatedly to remove products and unreacted substrates. The recovered PCN-222(Cu)@TR-1 was dried under vacuum and reused in next cycle under the same procedure.

**5. Free radical experiments**

In a typical reaction, PCN-222(Cu)TR-1 (10 mg) was used as catalyst, **1a** (0.1 mmol), **2a** (0.13 mmol) and TEMPO/benzoquinone (BQ)/$Na_2EDTA$/coumarin/$NaN_3$ (0.2 mmol) were dispersed in $CH_3CN$ (2 mL) in 5 mL branched Schlenk tube, which were kept for 10 hours under $O_2$ atmosphere. After the reaction was finished, the yield was determined by flash column chromatography.

# Section S2. Supporting Material Characterization Figures

## Figure S1. $^1$H NMR spectra of PCN-222(Cu) and PCN-222(Cu)-$NH_2$

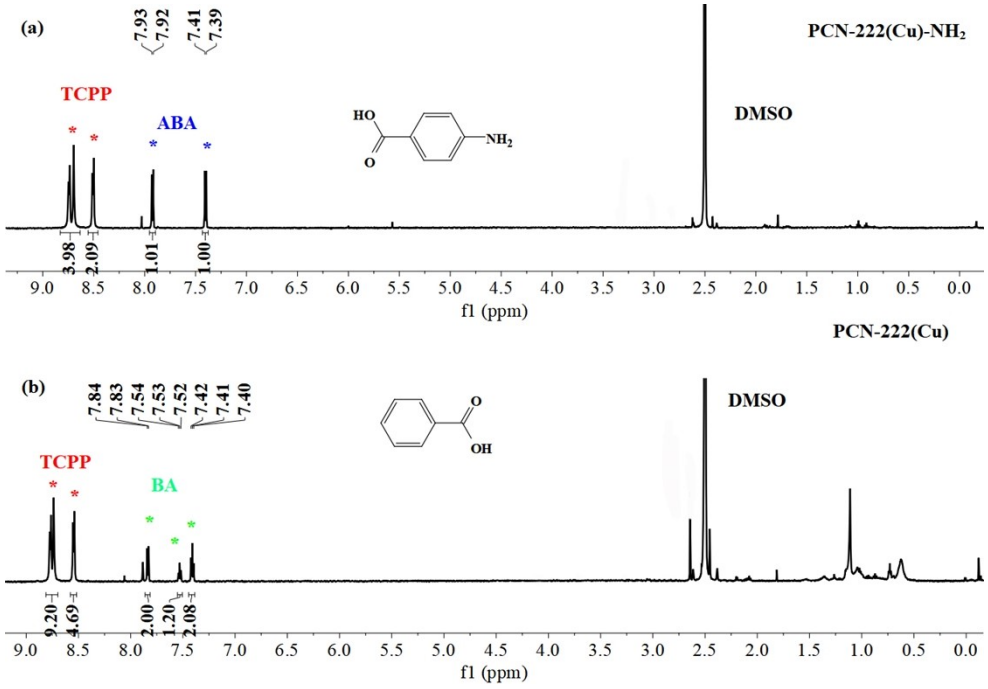


Based on the structure formula $C_{48}H_{32}N_4O_{16}Zr_3$ of PCN-222(Cu), the fuctionlization degree per Zr-oxo cluster can be obtained. Specifically, the content of TCPP was calculated to be 0.26, thus the content of the Zro cluster was 0.13, and the content of ABA was calculated to be 0.5. Therefore, the ratio was 3.8:1.

## Figure S2. XPS pattern of C 1s of the synthetic samples

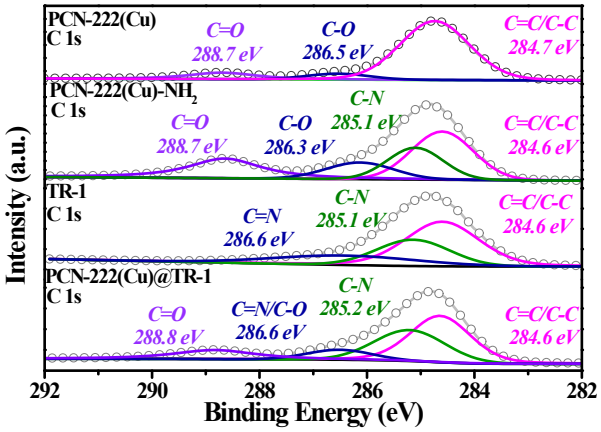

**Figure S3. XPS pattern of O 1s of the synthetic samples**

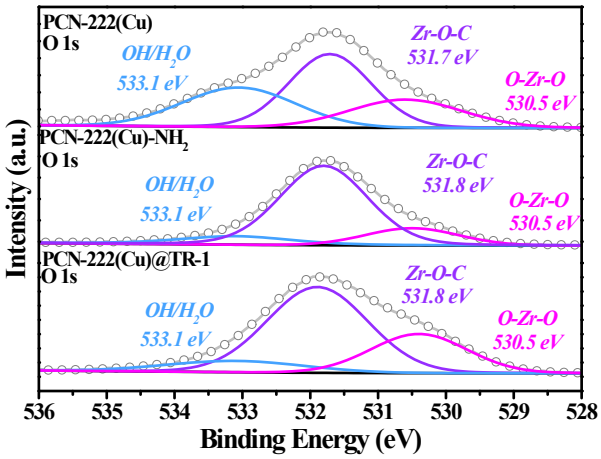


**Figure S4. XPS pattern of Zr 3d of the synthetic samples**

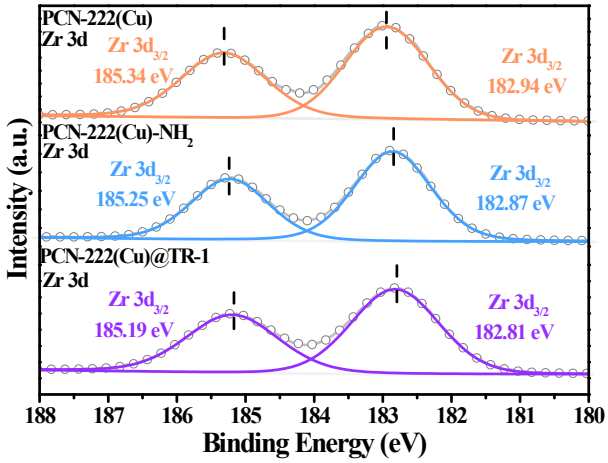


**Figure S5. XPS pattern of Cu 2p of the synthetic samples**

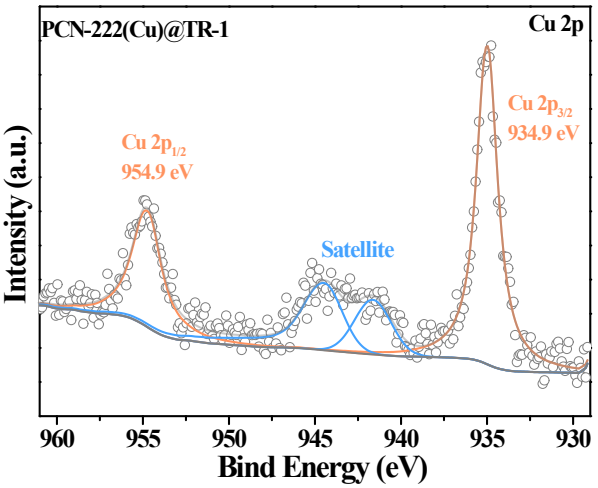

**Figure S6. SEM pattern of PCN-222(Cu)**

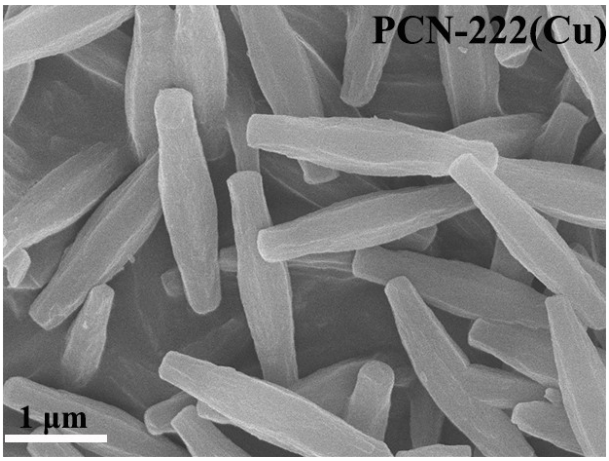


**Figure S7. SEM pattern of PCN-222(Cu)-$NH_2$**

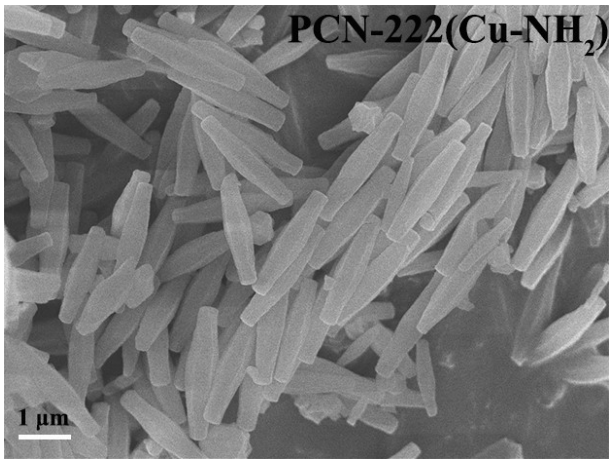


**Figure S8. SEM pattern of TR-1**

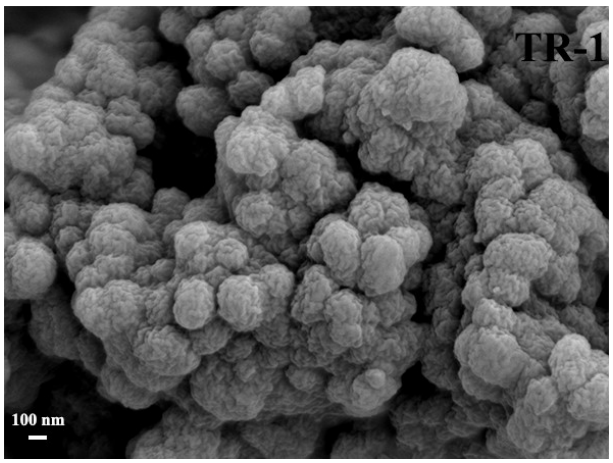

**Figure S9. TEM pattern of PCN-222(Cu)@TR-1**

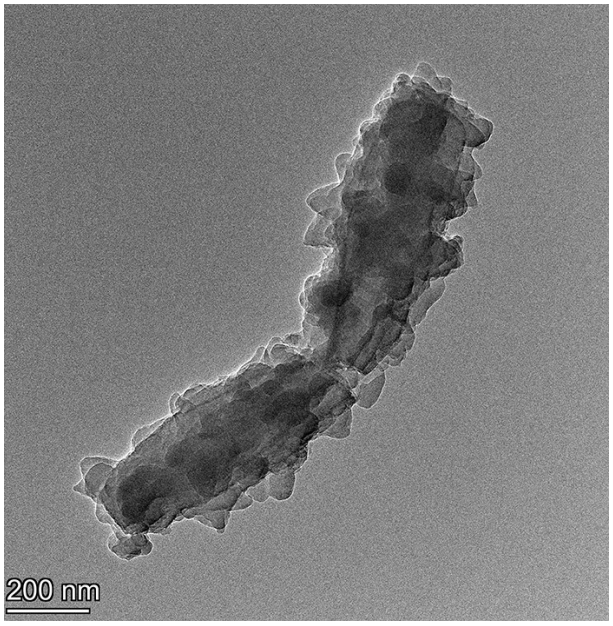


**Figure S10. Mapping pattern of PCN-222(Cu)@TR-1 sample.**

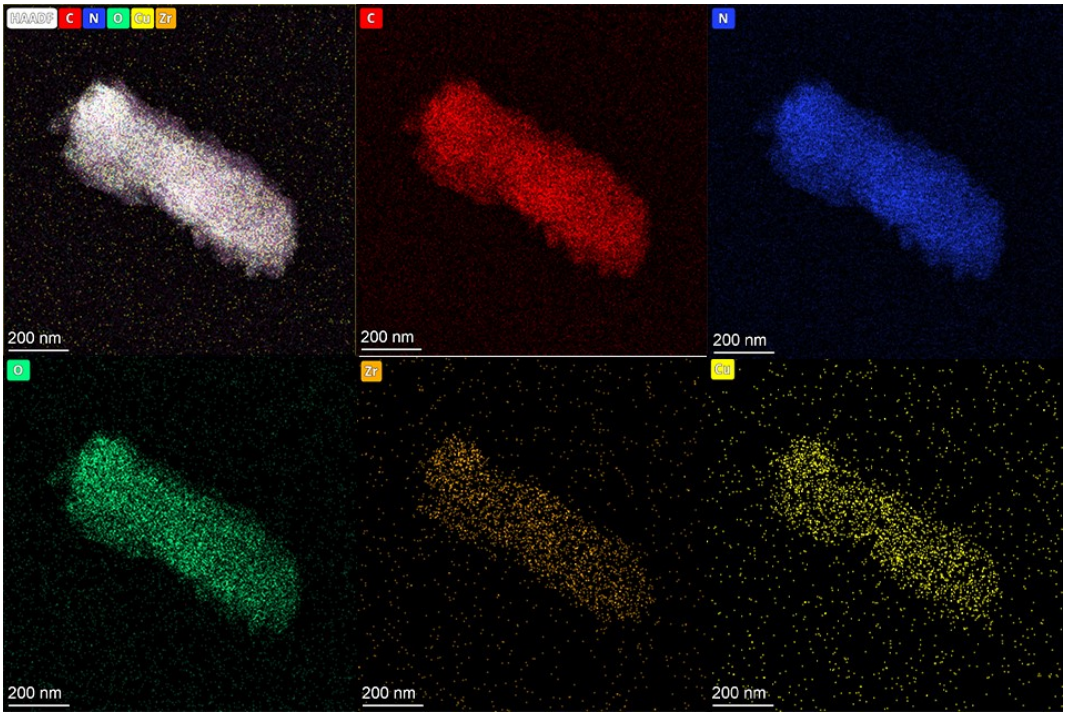


**Figure S11. $N_2$ adsorption isotherm of PCN-222(Cu) sample**

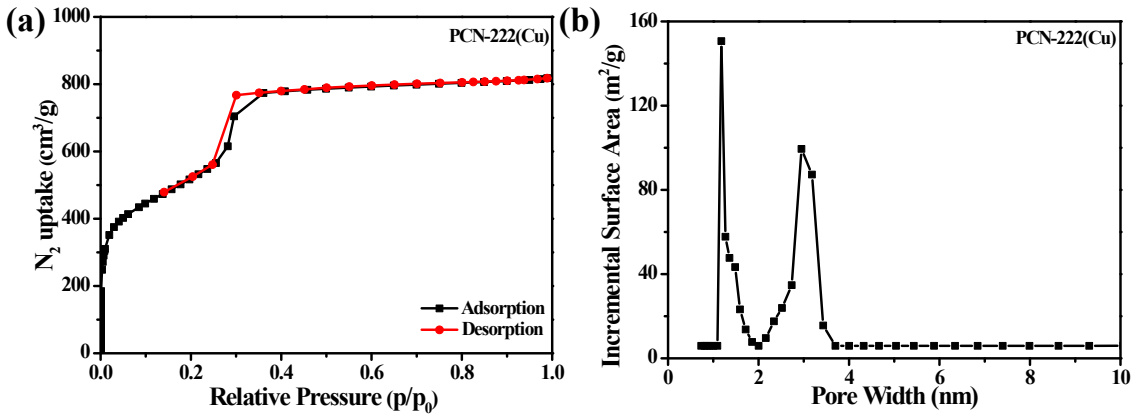


**Figure S12. $N_2$ adsorption isotherm of PCN-222(Cu)-$NH_2$ sample**

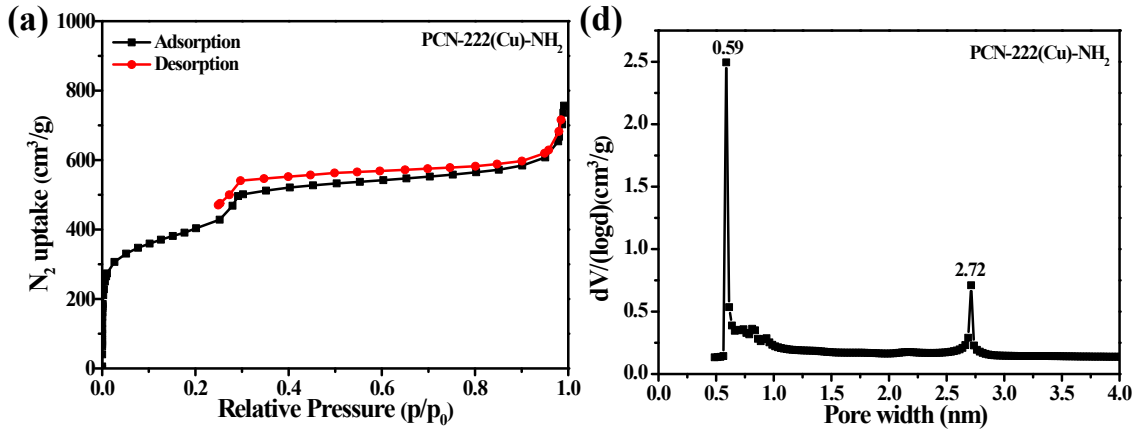


**Figure S13. $N_2$ adsorption isotherm of TR-1 sample**

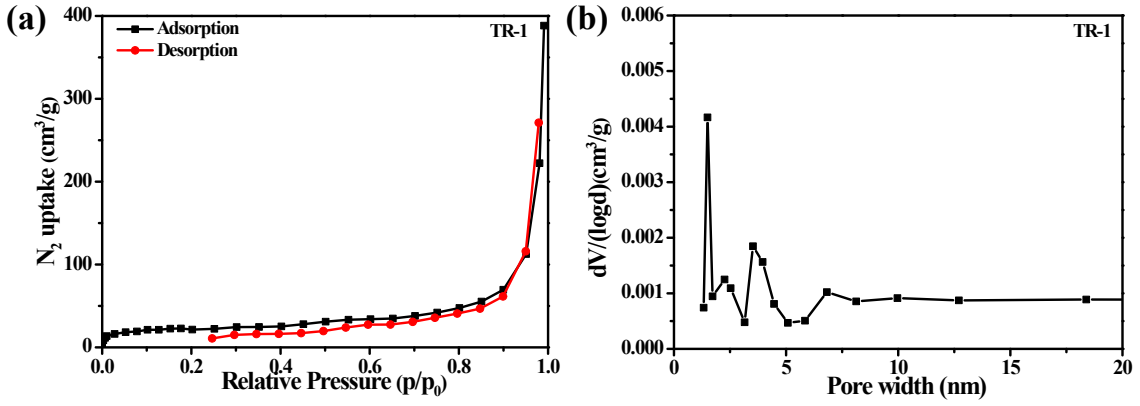


**Figure S14. $N_2$ adsorption isotherm of PCN-222(Cu)@TR-1 sample**

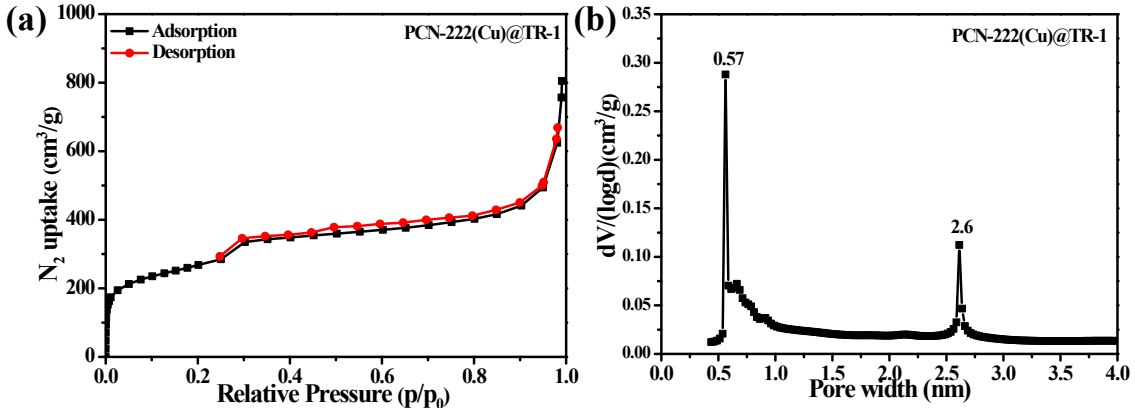


**Figure S15. Thermogravimetric analysis curve of the synthetic samples**

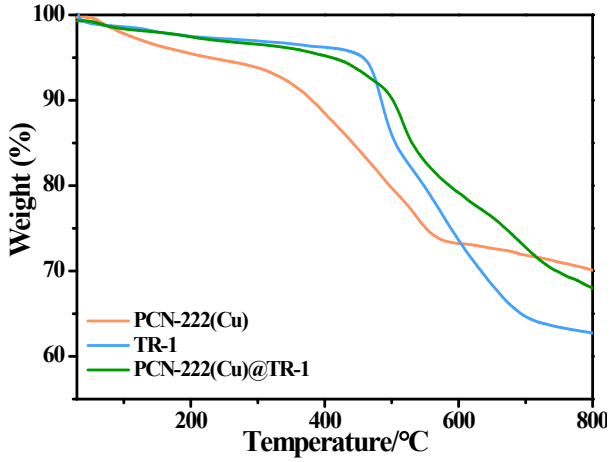


**Figure S16. (a) UV–vis DRS spectra of PCN-222(Cu)@TR-1 and physical mixing; (b)The optical band gaps pattern of the synthetic samples**

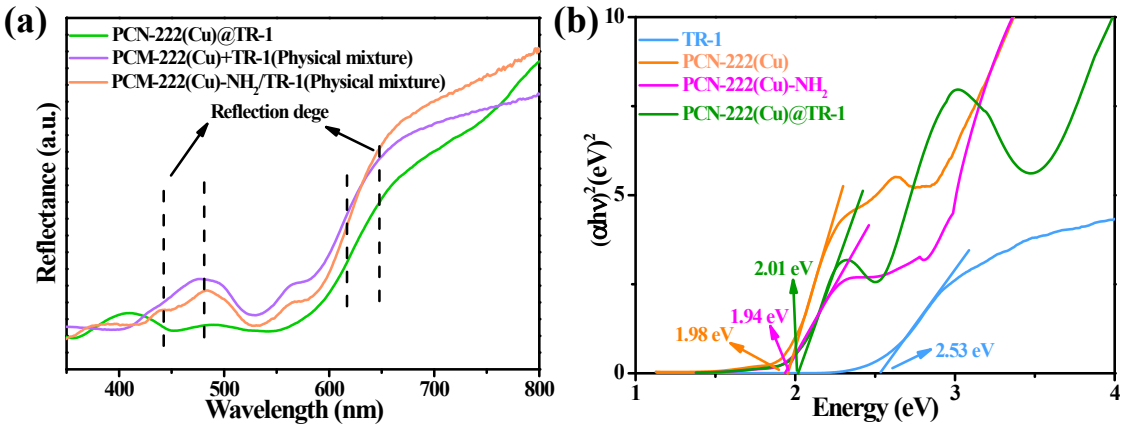


**Figure S17. Mott–Schottky patterns of the synthetic samples**

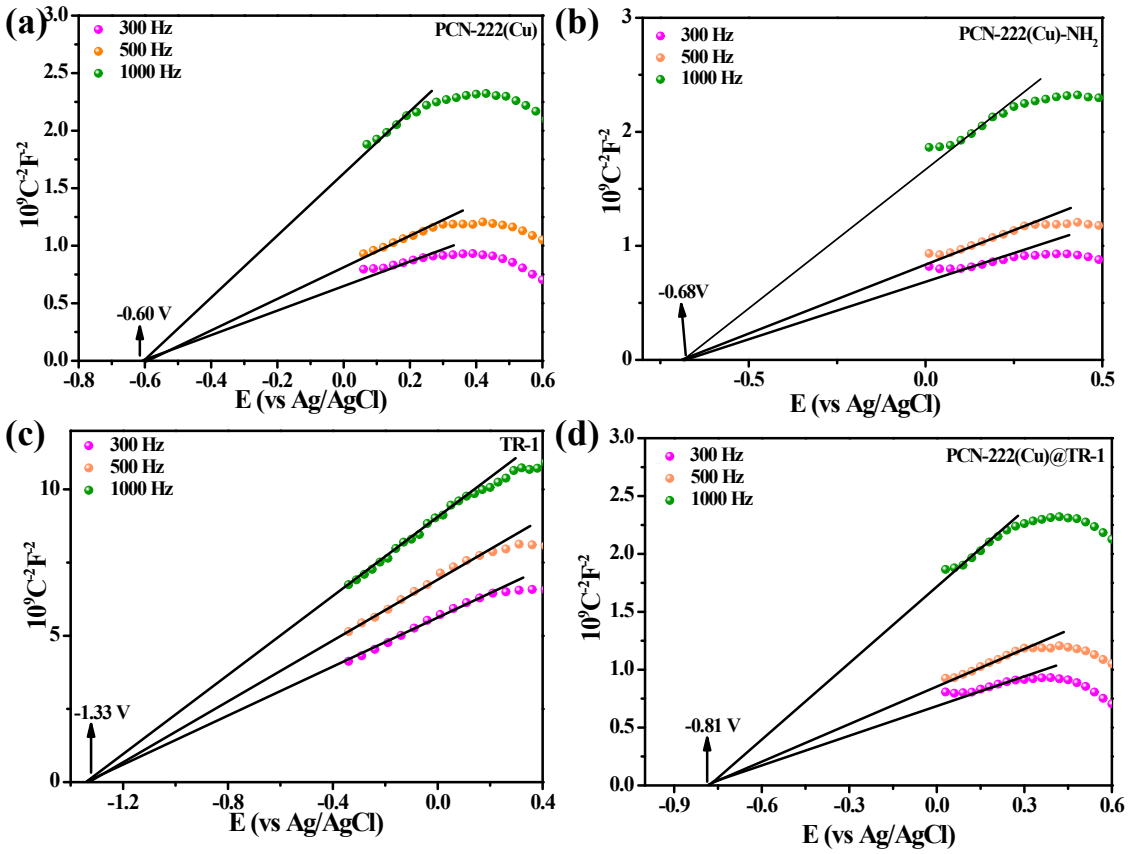


**Figure S18. (a) The ESR pattern for PCN-222(Cu)@TR-1 in dark and light; (b) Photoluminescence spectra of the synthetic samples**

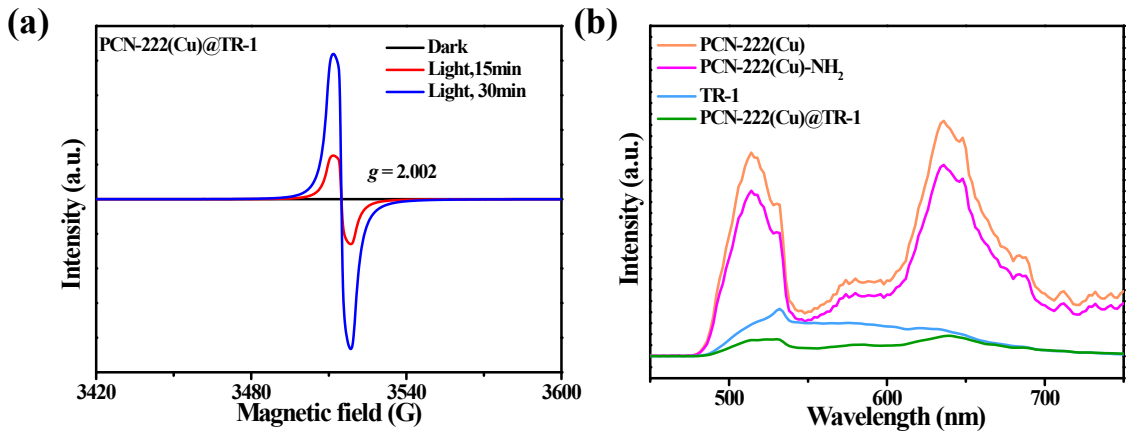

# Section S3. Catalytic Data

## Table S1. Optimization of the reaction conditions for aerobic photocatalytic C(sp$^3$)-C(sp$^2$) cross-dehydrogenative coupling reaction[a]

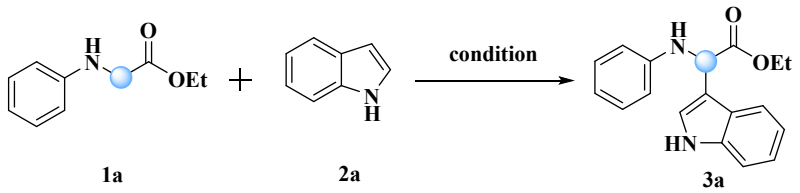


1a 2a 3a

| Entry | Catalyst | Sol. | light | Atmosphere | T/h | Yield[b]/% |
|---|---|---|---|---|---|---|
| 1 | **PCN-222(Cu)@TR-1** | **DMF** | √ | **$O_2$** | **10** | **20** |
| 2 | PCN-222(Cu)@TR-1 | **$CH_3CN$** | √ | **$O_2$** | **10** | **90** |
| 3 | PCN-222(Cu)@TR-1 | **DMSO** | √ | **$O_2$** | **10** | **Trace** |
| 4 | PCN-222(Cu)@TR-1 | **$CH_3Cl$** | √ | **$O_2$** | **10** | **23** |
| 5 | **PCN-222(Cu)@TR-1** | **Acetone** | √ | **$O_2$** | **10** | **20** |
| 6 | PCN-222(Cu)@TR-1 | **EtOH** | √ | **$O_2$** | **10** | **25** |
| 7 | PCN-222(Cu)@TR-1 | **THF** | √ | **$O_2$** | **10** | **16** |
| 8 | PCN-222(Cu)@TR-1 | **$CH_3CN$** | √ | **$N_2$** | **10** | **----** |
| 9 | **----** | **$CH_3CN$** | √ | **$O_2$** | **10** | **----** |
| 10 | PCN-222(Cu)@TR-1 | **$CH_3CN$** | × | **$O_2$** | **10** | **----** |
| 11[c] | PCN-222 | **$CH_3CN$** | √ | **$O_2$** | **10** | **28** |
| 12[d] | PCN-222(Fe) | **$CH_3CN$** | √ | **$O_2$** | **10** | **26** |
| 13[e] | PCN-222(Ni) | **$CH_3CN$** | √ | **$O_2$** | **10** | **15** |
| 14 | PCN-222(Cu) | **$CH_3CN$** | √ | **$O_2$** | **10** | **47** |
| 15 | PCN-222(Cu)-$NH_2$ | **$CH_3CN$** | √ | **$O_2$** | **10** | **55** |
| 16 | **TR-1** | **$CH_3CN$** | √ | **$O_2$** | **10** | **33** |
| 17[f] | PCN-222Cu+TR-1 | **$CH_3CN$** | √ | **$O_2$** | **10** | **56** |
| 18[g] | CuTPPM | **$CH_3CN$** | √ | **$O_2$** | **10** | **23** |

[*a*] Reaction condition: 1a (0.1 mmol), 2a (0.13 mmol), $CH_3CN$ (2 mL), room temperature, 300 W Xe Lamp, $O_2$ ball; [*b*] Isolated yields; [*c*] PCN-222 instead of PCN-222(Cu)@TR-1; [*d*] PCN-222(Fe) instead of PCN-222(Cu)@TR-1; [*e*] PCN-222(Ni) instead of PCN-222(Cu)@TR-1;[*f*] Physically mixed PCN-222(Cu) and TR-1; [*g*] CuTPPM instead of PCN-222(Cu)

## Figure S19. Wavelength-dependent AQE of aerobic photocatalytic C(sp$^3$)-

## C(sp$^2$) cross-dehydrogenative coupling reaction

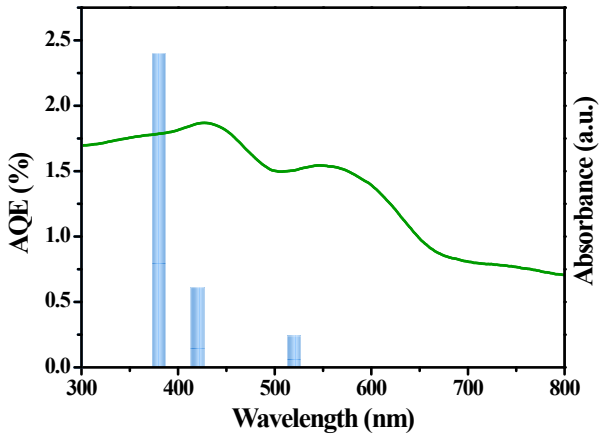


The test of apparent quantum efficiency (AQE) for aerobic photocatalytic C(sp$^3$)-C(sp$^2$) cross-dehydrogenative coupling reaction was measured as the reported literatures[6]. The different excited light sources to the reaction were investigated by different wavelengths (including 380 nm, 420 nm and 520 nm) at the illumination distance of 10 cm. Hence, the AQEs are estimated from the following equation:

$$AQE(\%) = \frac{number\ of\ product\ obtained}{number\ of\ incident\ obtained} \times 100\%$$

$$= \frac{n_p \times N_A}{\frac{P \times S \times t \times \lambda}{h \times c}} \times 100\%$$

$$= \frac{n_p \times N_A \times h \times c}{P \times S \times t \times \lambda} \times 100\%$$

where np is the mole number of product obtained (mol), $N_A$ is the Avogadro constant ($6.022 \times 10^{23}$ mol$^{-1}$), P is the optical density (W cm$^{-2}$), S is the light irradiation area (cm$^2$), t is the light irradiation time (s), λ is the monochromatic light wavelength (m), h is Planck's constant ($6.626 \times 10^{-34}$ J s), and c is the speed of light ($3 \times 10^8$ m s$^{-1}$).

## Table S3. The AQE of aerobic photocatalytic C(sp$^3$)-C(sp$^2$) cross-dehydrogenative coupling reaction

| λ (nm) | P (W cm$^-$ | AQE (%) |
|---|---|---|
| 380 | 12.8 | 2.4 |
| 420 | 27.2 | 0.61 |
| 520 | 30.3 | 0.24 |

**Figure S20. CV of 1a in dry acetonitrile solution with $Et_4NPF_6$ (0.1 M) at a scan rate of 50 mV/s**

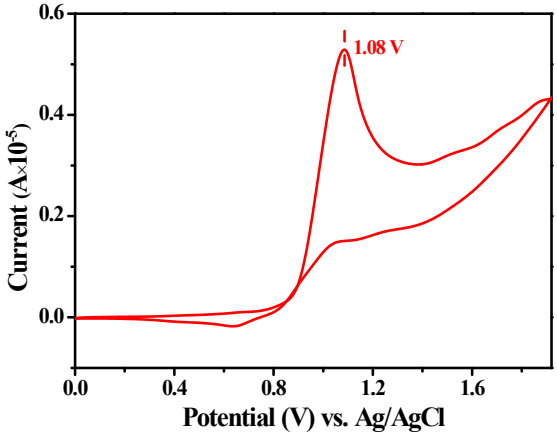


**Figure S21. Effect of scavengers on the aerobic photocatalytic $C(sp^3)-C(sp^2)$ cross-dehydrogenative coupling reaction**

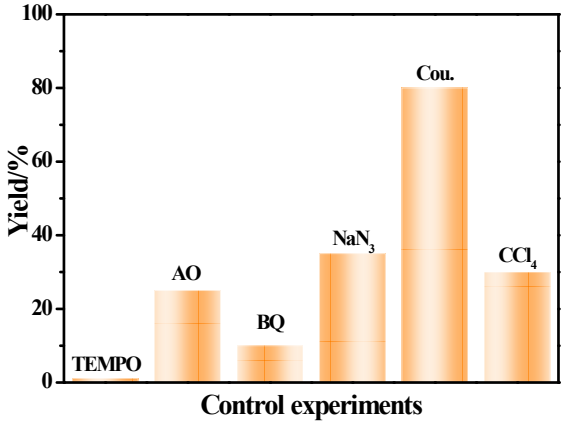


**Figure S22. (a) TEMP-$^1O_2$ spin-trapping EPR spectra; (b) DMPO-$O_2^{\bullet-}$ spin-trapping EPR spectra**

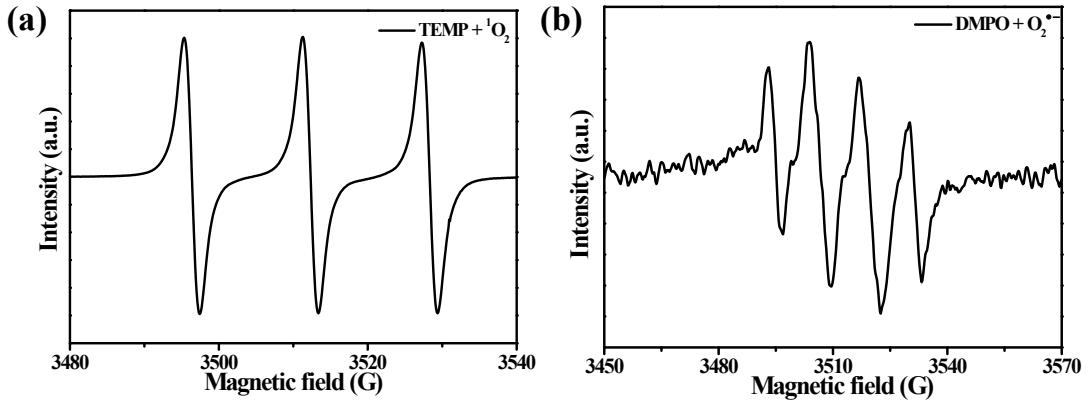

**Figure S23. Stepwise control experiments**

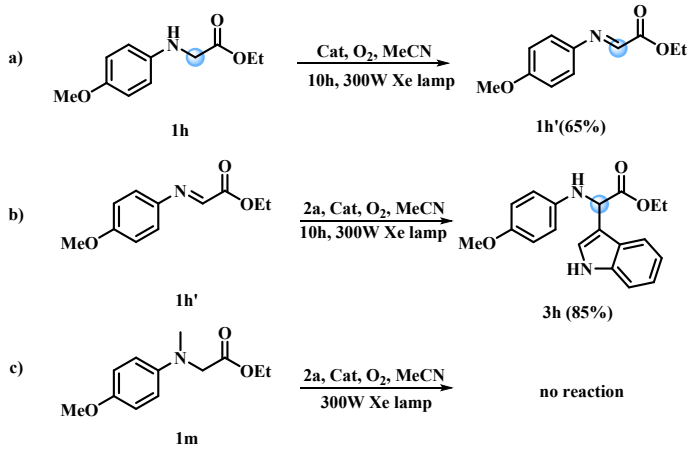


**Figure 24. $^1$H NMR spectrometry of imine intermediate**

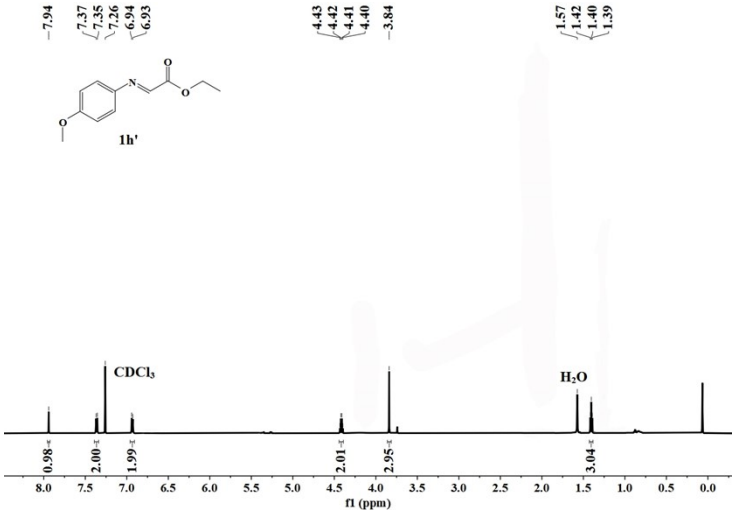


**Figure 25. High resolution mass spectrometry of imine intermediate and iminium ion**

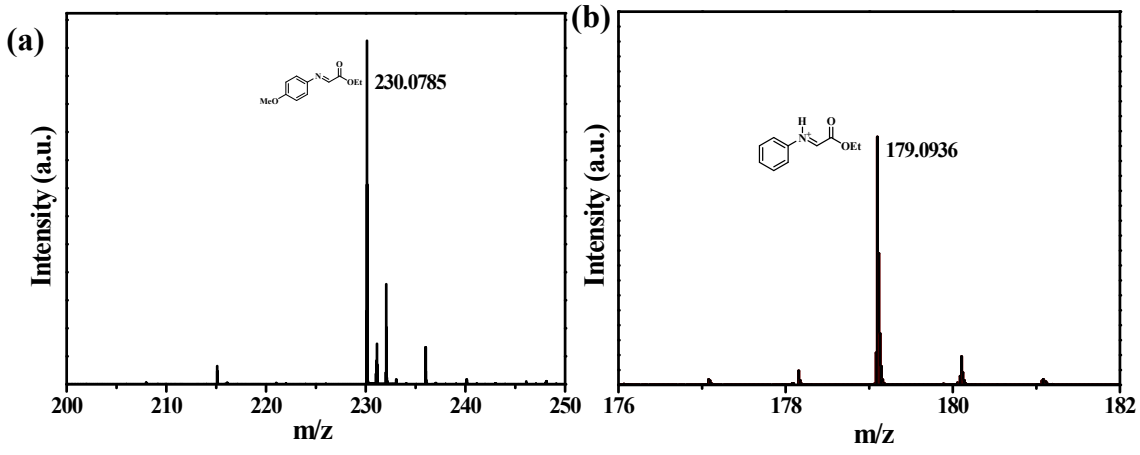

**Table S4. Fitting parameters of the fs-TAS decay traces of PCN-222(Cu), TR-1, and PCN-222(Cu)@TR-1 samples**

| Samples | $\tau_1$ (ps) | $\tau_2$ (ps) | $\tau_{ave}$ (ps) |
|---|---|---|---|
| PCN-222(Cu) | 2.7 | 27.81 | 30.58 |
| TR-1 | 1.39 | 64 | 61.92 |
| PCN-222(Cu)@TR-1 | 0.37 | 195.54 | 193.84 |

**Table S5. Comparison of PCN-222(Cu)@TR-1 with previous reports for the synthsis of glycine derivatives**

| Entry | Cat. | t/h | Yield/% | TOF($h^{-1}$) | Ref. |
|---|---|---|---|---|---|
| 1 | $[Ir(ppy)_2bpy]PF_6$+$Zn(OAC)_2$ (10mol%) | 48 | 72 | 0.15 | 7 |
| 2 | CuCl (5mol%) | 6 | 86 | 2.86 | 8 |
| 3 | $Fe(ClO_4)_3$ (10mol%) | 10 | 62 | 0.62 | 9 |
| 4 | Ru-COF+ $Zn(OAC)_2$ (10mol%) | 35 | 95 | 0.27 | 10 |
| ***5*** | ***PCN-222(Cu)@TR-1 (1.64mol%)*** | ***10*** | ***90*** | ***5.48*** | ***Our work*** |

## Section S4. Catalyst Stability Characterization

**Figure 26. (a) Hot filtration test (b) Recycling experiments**

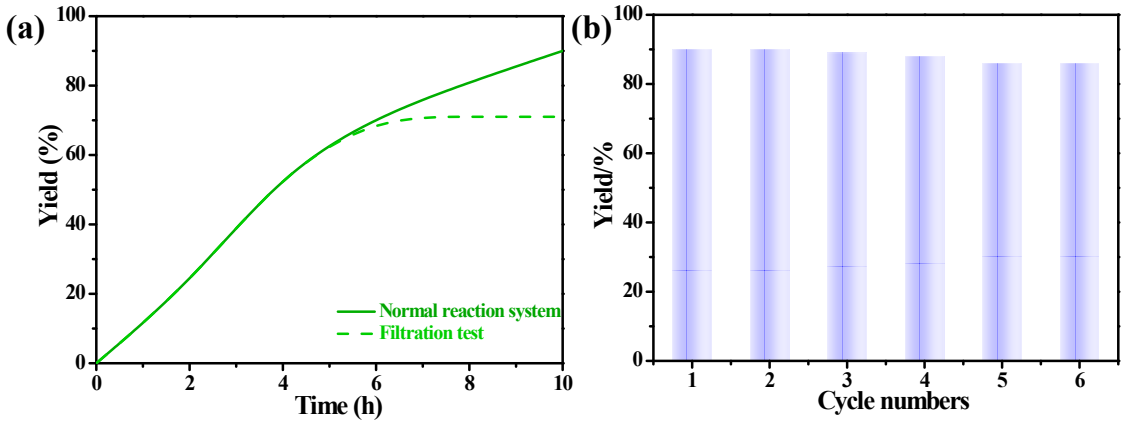


**Figure 27. IR and PXRD patterns for PCN-222(Cu)@TR-1 of the as-synthesized sample and after the 6th runs of the addition reactions**

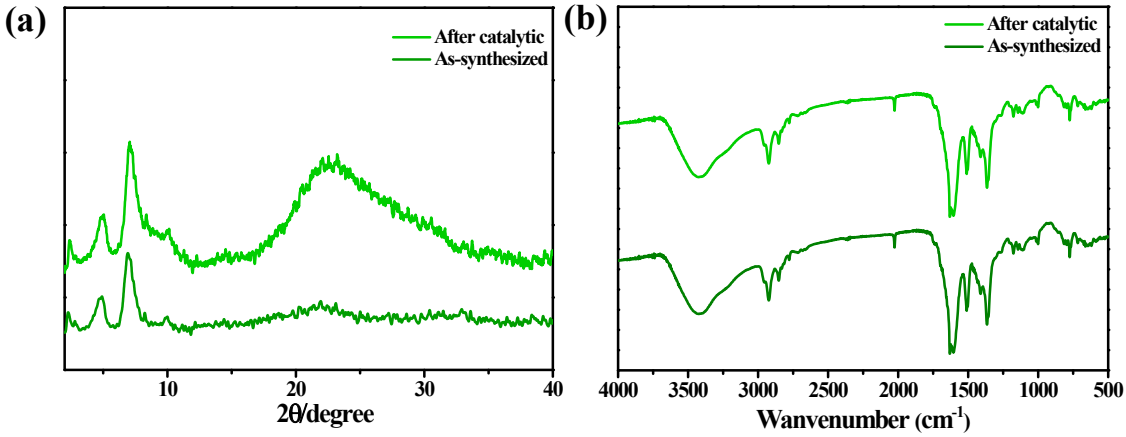


**Figure 28. SEM of PCN-222(Cu)@TR-1 after catalysis**

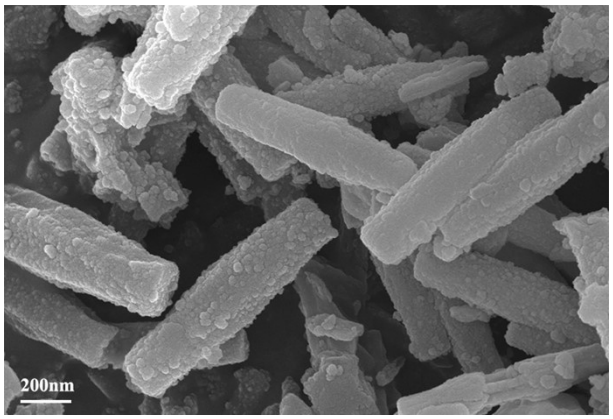

**Figure 29. XPS pattern for PCN-222(Cu)@TR-1 of the as-synthesized sample and after the 6th runs of the addition reactions**

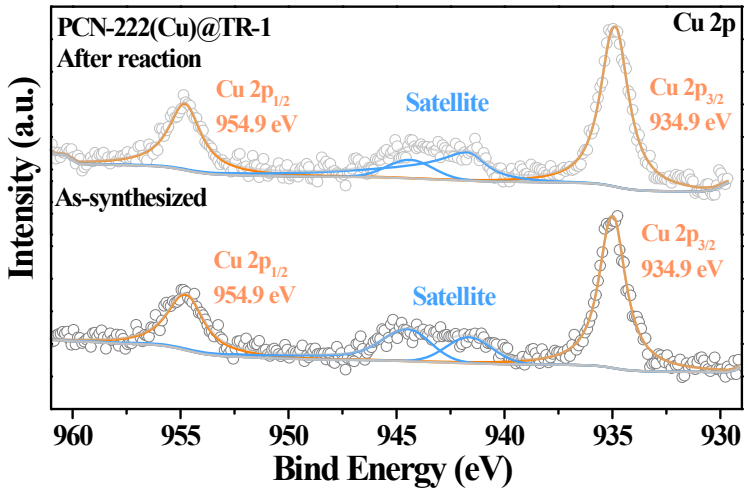

# Section S5. NMR, HRMS Data of Products

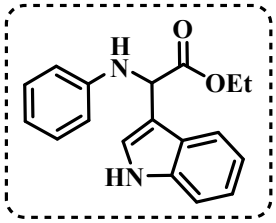

**Ethyl 2-(1H-indol-3-yl)-2-(phenylamino) acetate (3a)[11]**

**Brownish oil. $^1$H NMR** (600 MHz, $CDCl_3$) δ 8.15 (s, 1H), 7.84 (d, J = 8.0 Hz, 1H), 7.37 (d, J = 8.1 Hz, 1H), 7.24 - 7.12 (m, 5H), 6.73 (m, 1H), 6.65 (d, J = 7.8 Hz, 2H), 5.40 (s, 1H), 4.77 (s, 1H), 4.29-4.26 (m, 1H), 4.19 - 4.10 (m, 1H), 1.23 (t, J = 7.1 Hz, 3H). **$^{13}$C NMR** (151MHz, $CDCl_3$) *δ* 172.58, 146.57, 136.52, 129.28, 125.84, 123.09, 122.56, 120.05, 119.62, 118.08, 113.41, 112.67, 111.39, 61.61, 54.29, 14.16. **HRMS** (ESI-TOF): calculated for $C_{18}H1_8N_2O_2$ ($M+Na^+$) requires 317.1260, found 317.1258.

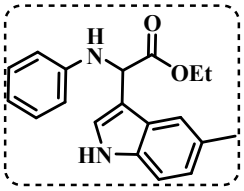

**Ethyl 2-(5-methyl-1H-indol-3-yl)-2-(phenylamino)acetate (3b)**

**Brownish oil**. **$^1$H NMR** (600 MHz, $CDCl_3$) δ 8.05 (d, *J* = 11.4 Hz, 1H), 7.62 (s, 1H), 7.25 -7.15 (m, 4H), 7.06 (d, *J* = 8.5 Hz, 1H), 6.73 (t, *J* = 7.3 Hz, 1H), 6.67 - 6.64 (m, 2H), 5.37 (s, 1H), 4.72 (s, 1H), 4.28 (m, 1H), 4.15 (m, 1H), 2.48 (s, 3H), 1.24 (d, *J* = 7.1 Hz, 3H). **$^{13}$C NMR** (151 MHz, $CDCl_3$) δ 172.67, 146.63, 134.82, 129.25, 126.06, 124.21, 123.19, 119.18, 118.05, 113.38, 112.07, 111.03, 61.56, 54.29 , 21.55, 14.19. **HRMS** (ESI-TOF): calculated for $C_{19}H_{20}N_2O_2$ ($M+Na^+$) requires 331.1417, found 331.1416.

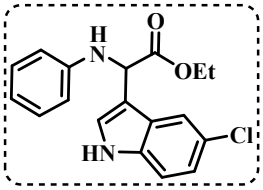

**Ethyl 2-(5-chloro-1H-indol-3-yl)-2-(phenylamino)acetate (3c)**

**Yellow liquid. $^1$H NMR (600 MHz, $CDCl_3$)** δ 8.22 (s, 1H), 7.82 (d, *J* = 1.9 Hz, 1H), 7.20 (d, *J* = 1.5 Hz, 1H), 7.18 - 7.15 (m, 4H), 6.74 (t, *J* = 7.3 Hz, 1H), 6.63 (d, *J* = 8.6 Hz, 2H), 5.33 (s, 1H), 4.79 (s, 1H), 4.29 - 4.46 (m, 1H), 4.17 - 4.14 (m, 1H), 1.23 (t, *J* = 7.1 Hz, 3H). **$^{13}$C NMR (151 MHz, $CDCl_3$)** δ 172.27, 146.33, 134.90, 129.30, 126.85, 125.83, 124.47, 122.90, 119.22, 118.62, 118.25, 113.47, 112.43 , 61.84, 54.14, 14.12. **HRMS** (ESI-TOF): calculated for $C_{18}H_{17}ClN_2O_2$ ($M+Na^+$) requires 351.0871, found 351.0870.

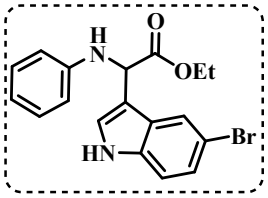

**Ethyl 2-(5-bromo-1H-indol-3-yl)-2-(phenylamino)acetate (3d)**

**Yellow liquid.**

**$^1$H NMR (600 MHz, $CDCl_3$)** δ 8.31 (s, 1H), 7.99 (s, 1H), 7.29 (d, *J* = 8.6 Hz, 1H), 7.19 - 7.14 (m, 4H), 6.75 (t, *J* = 7.4 Hz, 1H), 6.63 (d, *J* = 8.1 Hz, 2H), 5.33 (s, 1H), 4.77 (s, 1H), 4.27 (m, 1H), 4.16 - 4.13 (m, 1H), 1.26 - 1.23 (m, 3H). **$^{13}$C NMR (151 MHz, $CDCl_3$)** δ 172.35, 146.35, 135.21, 129.34, 125.92, 125.41, 124.94, 122.23, 121.64, 118.65, 118.29, 115.27, 113.49, 112.97, 61.91, 54.15, 14.13. **HRMS** (ESI-TOF): calculated for $C_{18}H_{17}BrN_2O_2$ ($M+Na^+$) requires 395.0366, found 395.0367.

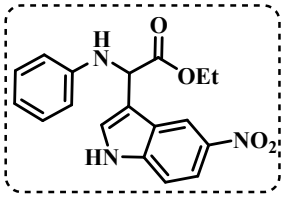

**Ethyl 2-(5-nitro-1H-indol-3-yl)-2-(phenylamino)acetate (3e)**

**Brownish liquid.** $^1$H NMR (600 MHz, $CDCl_3$) δ 8.86 (s, 1H), 8.75 (d, *J* = 21.6 Hz, 1H), 8.13 (d, *J* = 8.9 Hz, 1H), 7.44 - 7.36 (m, 2H), 7.15 (t, *J* = 7.8 Hz, 2H), 6.75 (t, *J* = 7.3 Hz, 1H), 6.63 (d, *J* = 7.9 Hz, 2H), 5.43 (s, 1H), 4.92 (s, 1H), 4.28 (m, 1H), 4.21 - 4.11 (m, 1H), 1.24 (t, *J* = 7.1 Hz, 3H). $^{13}$C NMR (151 MHz, $CDCl_3$) δ 171.87, 146.07, 141.95, 139.67, 129.37, 126.42, 125.19, 118.51, 118.12, 117.24, 115.32, 113.58, 111.61, 62.21, 54.07, 14.06. **HRMS** (ESI-TOF): calculated for $C_{18}H_{17}N_3O_2$ ($M+Na^+$) requires 332.1111, found 362.1109.

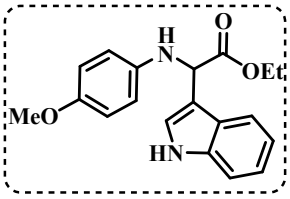

**Ethyl 2-(1H-indol-3-yl)-2-((4-methoxyphenyl)amino)acetate (3h)**

**Brownish oil. $^1$H NMR (600 MHz, $CDCl_3$)** δ 8.32 (s, 1H), 7.89 (d, *J* = 7.9 Hz, 1H), 7.41 (d, *J* = 8.0 Hz, 1H), 7.31 - 7.21 (m, 3H), 6.81 (d, *J* = 8.5 Hz, 2H), 6.68 (d, *J* = 8.6 Hz, 2H), 5.40 (s, 1H), 4.31 (m, 1H), 4.19 (m, 1H), 3.79 (s, 3H), 1.27 (t, *J* = 7.1 Hz, 3H). **$^{13}$C NMR (151 MHz, $CDCl_3$)** δ 172.87, 152.54, 140.82, 136.49, 125.87, 123.07, 122.51, 120.01, 119.58 116.60, 114.86, 112.77, 111.42, 61.53, 55.73, 55.24, 14.17. **HRMS** (ESI-TOF): calculated for $C_{19}H_{20}N_2O_3$ ($M+Na^+$) requires 347.1366, found 347.1365.

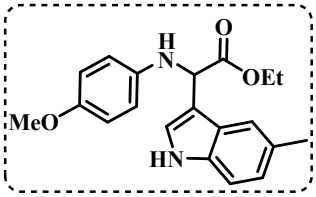

**Ethyl 2-((4-methoxyphenyl)amino)-2-(5-methyl-1H-indol-3-yl)acetate (3i)**

**Brownish oil. $^1$H NMR (600 MHz, $CDCl_3$)** δ 8.10 (s, 1H), 7.61 (s, 1H), 7.25 (d, *J* = 6.8 Hz, 1H), 7.19 (d, *J* = 2.4 Hz, 1H), 7.06 (d, *J* = 8.3 Hz, 1H), 6.76 (d, *J* = 8.9 Hz, 2H), 6.63 (d, *J* = 8.9 Hz, 2H), 5.30 (s, 1H), 4.47 (s, 1H), 4.27 - 4.26 (m, 1H), 4.16 - 4.10 (m, 1H), 3.73 (s, 3H), 2.47 (s, 3H), 1.23 (t, *J* = 7.1 Hz, 3H). **$^{13}$C NMR (151 MHz, $CDCl_3$)** δ 172.90, 152.53, 140.89, 134.80, 129.37, 126.10, 124.19, 123.11, 119.16, 114.84, 112.30, 111.02, 61.46, 55.75, 55.24, 21.56, 14.16. **HRMS** (ESI-TOF): calculated for $C_{20}H_{22}N_2O_3$ ($M+Na^+$) requires 361.1523, found 361.1523.

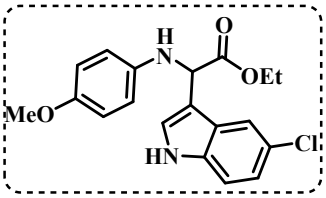

**Ethyl 2-(5-chloro-1H-indol-3-yl)-2-((4-methoxyphenyl)amino)acetate (3j)**

**Yellow liquid. $^1$H NMR** (600 MHz, $CDCl_3$) δ 8.36 (s, 1H), 7.87 (s, 1H), 7.33 - 7.19 (m, 3H), 6.80 (d, *J* = 6.9 Hz, 2H), 6.66 (d, *J* = 8.6 Hz, 2H), 5.32 (s, 1H), 4.30 (m, 1H), 4.20 (m, 1H), 3.78 (s, 3H), 1.28 (t, *J* = 7.0 Hz, 3H). **$^{13}$C NMR** (151 MHz, $CDCl_3$) δ 172.53, 152.64, 140.56, 134.88, 126.90, 125.80, 124.42, 122.88, 119.19, 114.91, 112.43, 61.73, 55.75, 55.10, 14.13. **HRMS** (ESI-TOF): calculated for $C_{19}H_{19}ClN_2O_3$ ($M+Na^+$) requires 381.0976, found 381.0975.

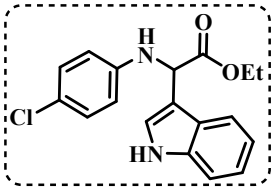

**Ethyl 2-((4-chlorophenyl)amino)-2-(1H-indol-3-yl)acetate1-(3-chlorophenyl)-2-thiocyanat oethanone (3k)**

**Yellow liquid.** $^1$H NMR (600 MHz, $CDCl_3$) δ 8.17 (s, 1H), 7.81 (d, *J* = 8.0 Hz, 1H), 7.39 (d, *J* = 8.1 Hz, 1H), 7.23 (m, 2H), 7.18 (t, *J* = 7.5 Hz, 1H), 7.08 (d, *J* = 8.8 Hz, 2H), 6.55 (d, *J* = 8.8 Hz, 2H), 5.34 (d, *J* = 5.9 Hz, 1H), 4.81 (d, *J* = 5.9 Hz, 1H), 4.24 - 4.27 (m, 1H), 4.12 - 4.15 (m, 1H), 1.22 (t, *J* = 7.1 Hz, 3H). **HRMS** (ESI-TOF): calculated for $C_{18}H_{17}ClN_2O_2$ ($M+Na^+$) requires 351.0871, found 351.0870.

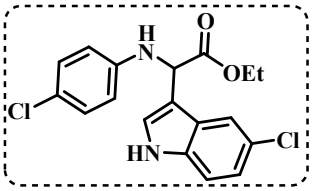


**Ethyl 2-(5-chloro-1H-indol-3-yl)-2-((4-chlorophenyl)amino)acetate (3l)**

**Yellow liquid.** $^{1}$H NMR (600 MHz, $CDCl_3$) δ 8.11 (s, 1H), 7.73 (d, *J* = 1.7 Hz, 1H), 7.23 (d, *J* = 8.6 Hz, 1H), 7.18 (d, *J* = 2.4 Hz, 1H), 7.12 (m, 1H), 7.01 (d, *J* = 8.8 Hz, 2H), 6.47 (d, *J* = 8.8 Hz, 2H), 5.21 (d, *J* = 5.8 Hz, 1H), 4.76 (d, *J* = 5.4 Hz, 1H), 4.22 - 4.18 (m, 1H), 4.11 - 4.03 (m, 1H), 1.17 (t, *J* = 7.1 Hz, 3H). $^{13}$C NMR (151 MHz, $CDCl_3$) δ 171.93, 144.80, 129.10, 126.78, 125.98, 124.40, 123.07, 119.21, 114.54, 112.43, 61.95, 54.12, 14.11. **HRMS** (ESI-TOF): calculated for $C_{18}H_{16}Cl_2N_2O_2$ ($M+Na^+$) requires 385.0481, found 385.0481.

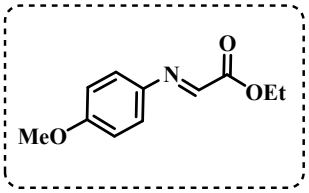


**Ethyl (E)-2-((4-methoxyphenyl)imino)acetate (3h', Known compound)[12]**

**Yellow oil.** $^{1}$H NMR (600 MHz, $CDCl_3$) δ 7.94 (s, 1H), 7.37 (d, J = 8.9 Hz, 2H), 6.94 (d, J = 8.9 Hz, 2H), 4.42 (q, J = 7.1 Hz, 2H), 3.84 (s, 3H), 1.41 (t, J = 7.1 Hz, 3H). **HRMS** (ESI-TOF): calculated for $C_{18}H_{16}Cl_2N_2O_2$ ($M+Na^+$) requires 230.07881, found 230.0785.

# Section S6. NMR Spectra of Products

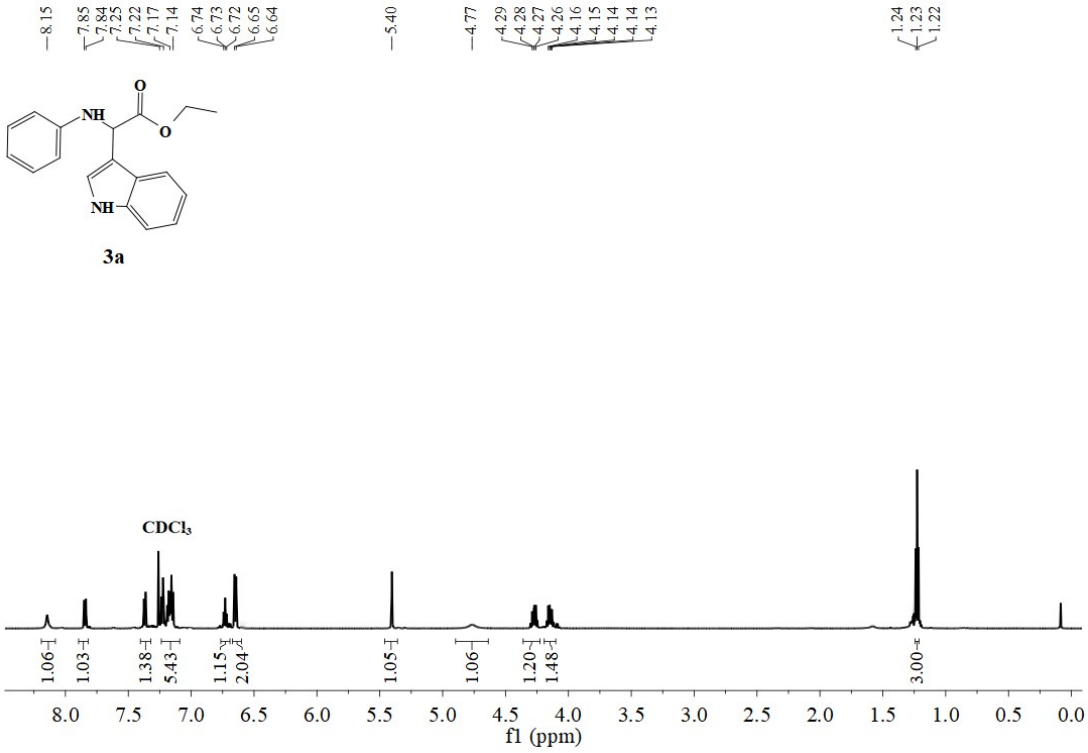


$^{1}$H NMR (600 MHz, $CDCl_3$) spectrum for **3a**

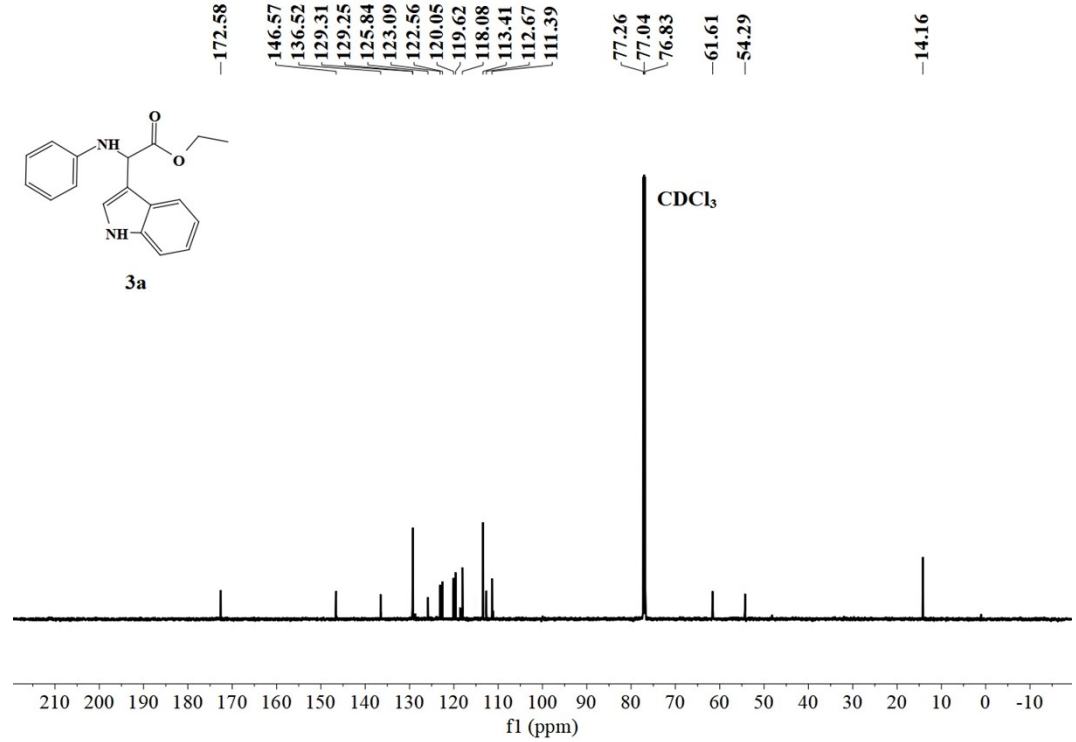


$^{13}$C NMR (151 MHz, $CDCl_3$) spectrum for **3a**

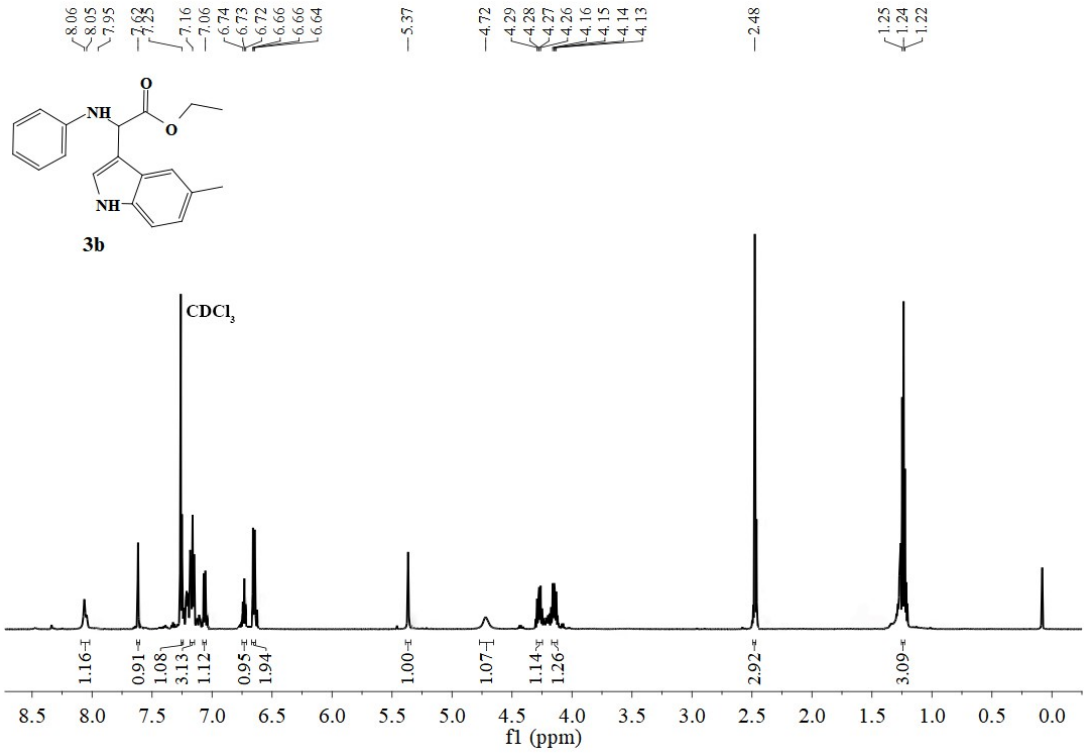


$^{1}$H NMR (600 MHz, $CDCl_3$) spectrum for **3b**

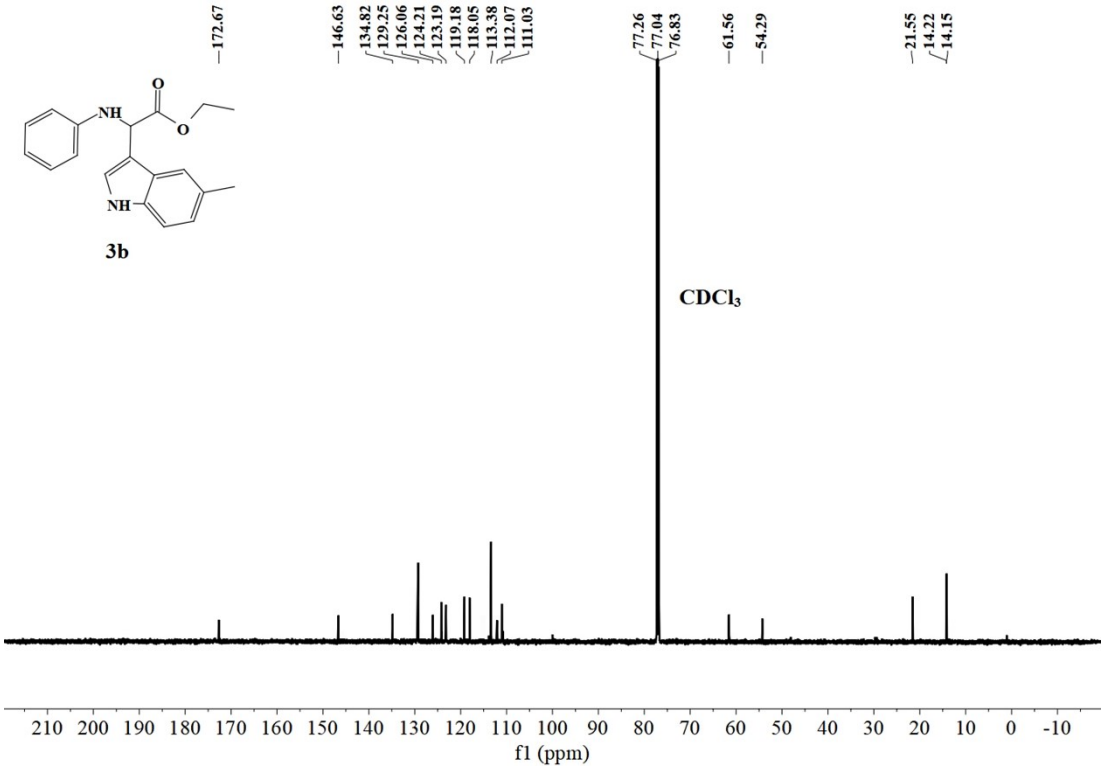


$^{13}$C NMR (151 MHz, $CDCl_3$) spectrum for **3b**

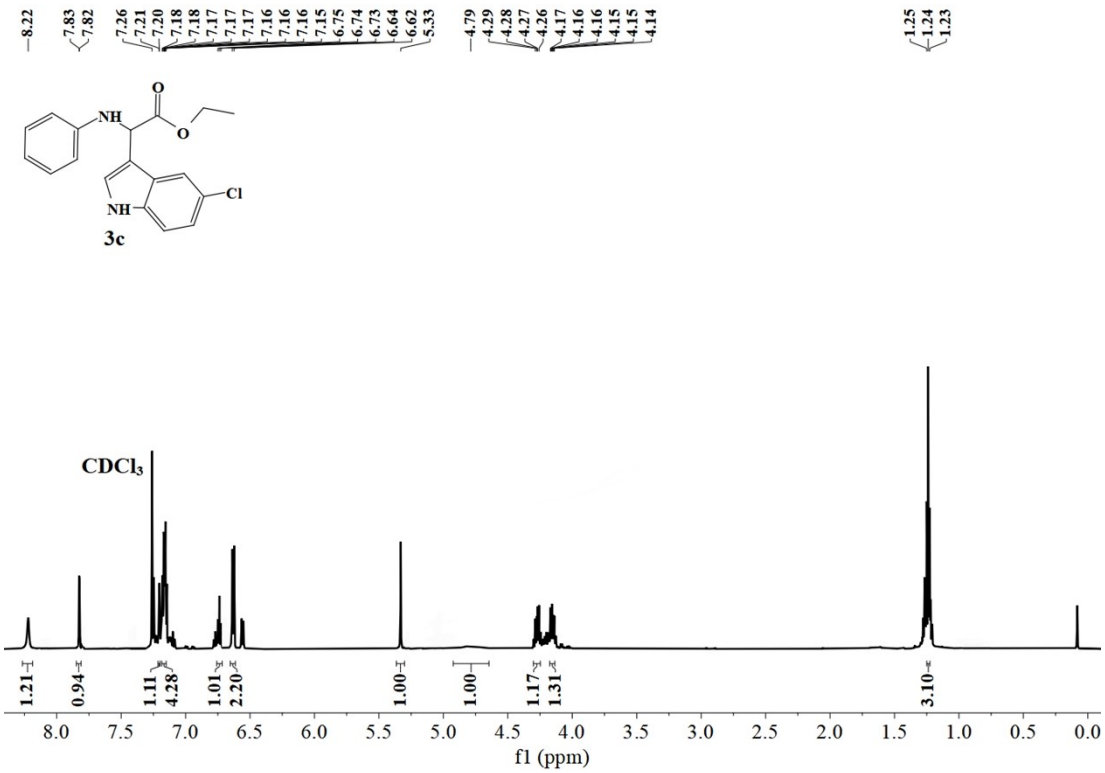


$^{1}$H NMR (600 MHz, $CDCl_3$) spectrum for **3c**

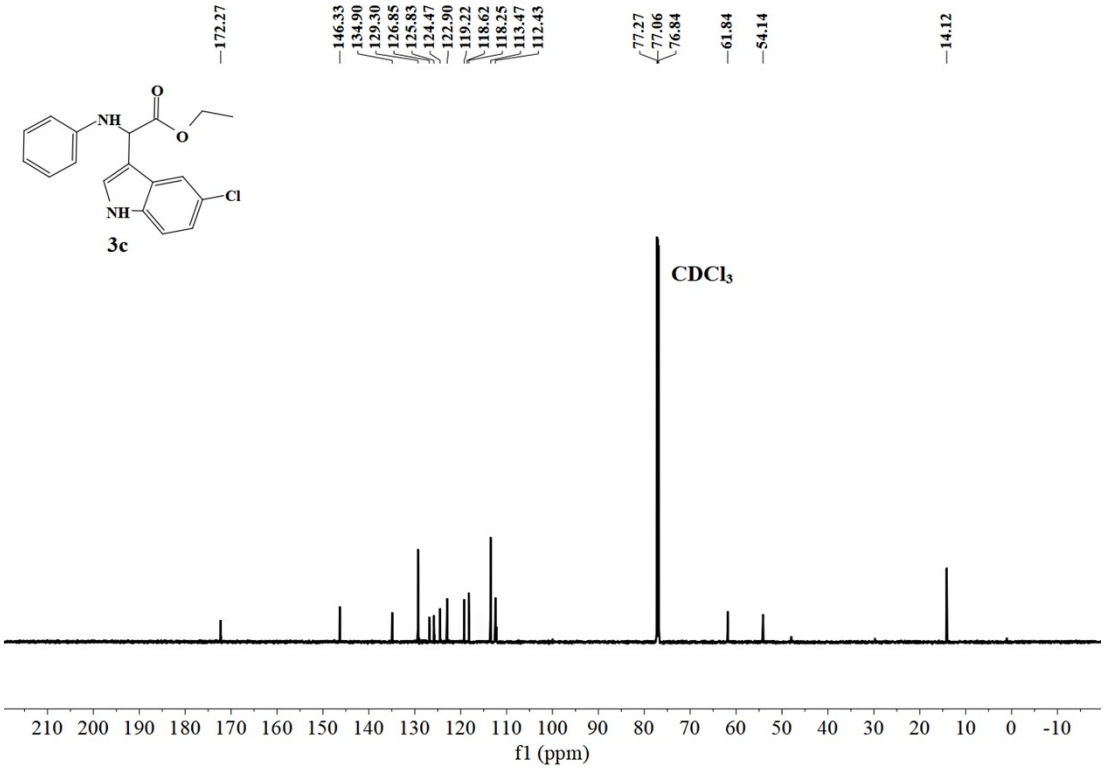


$^{13}$C NMR (151 MHz, $CDCl_3$) spectrum for **3c**

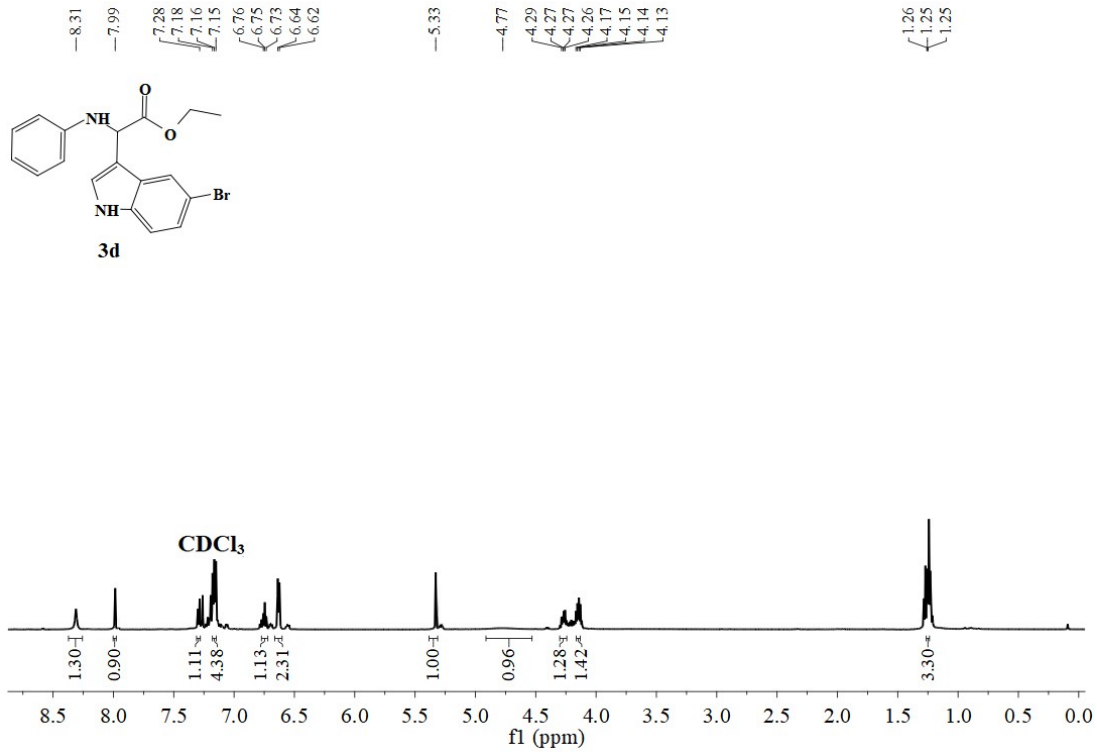


$^{1}$H NMR (600 MHz, $CDCl_3$) spectrum for **3d**

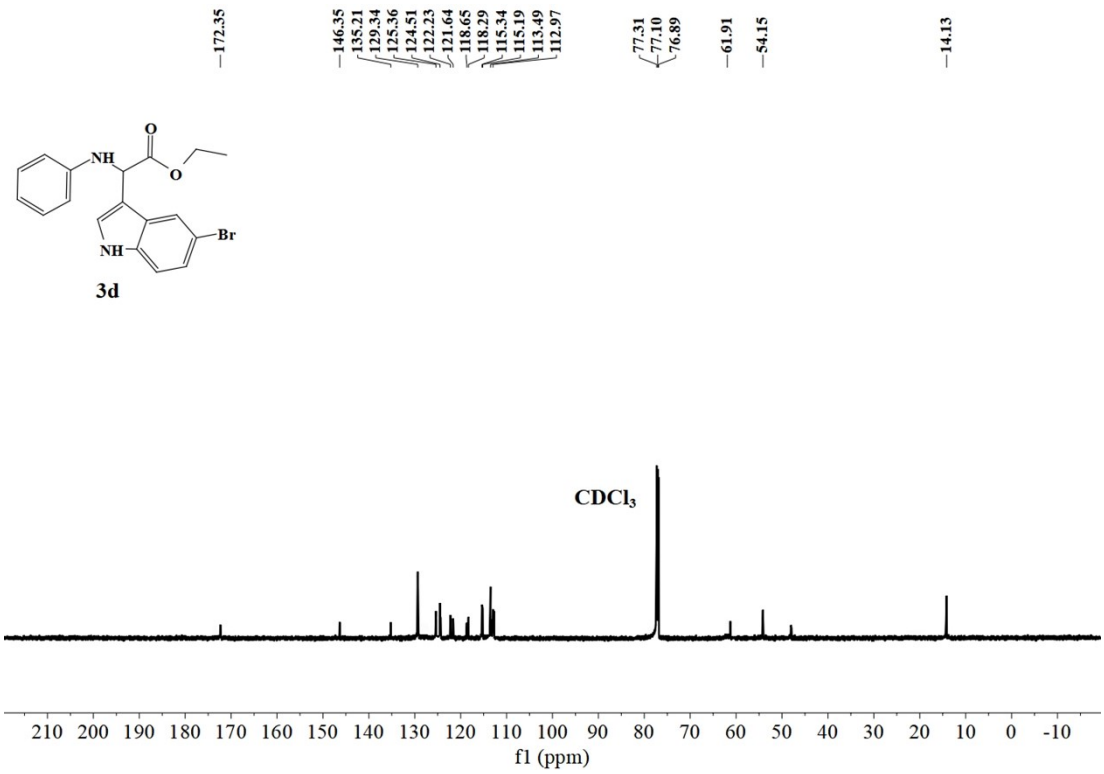


$^{13}$C NMR (151 MHz, $CDCl_3$) spectrum for **3d**

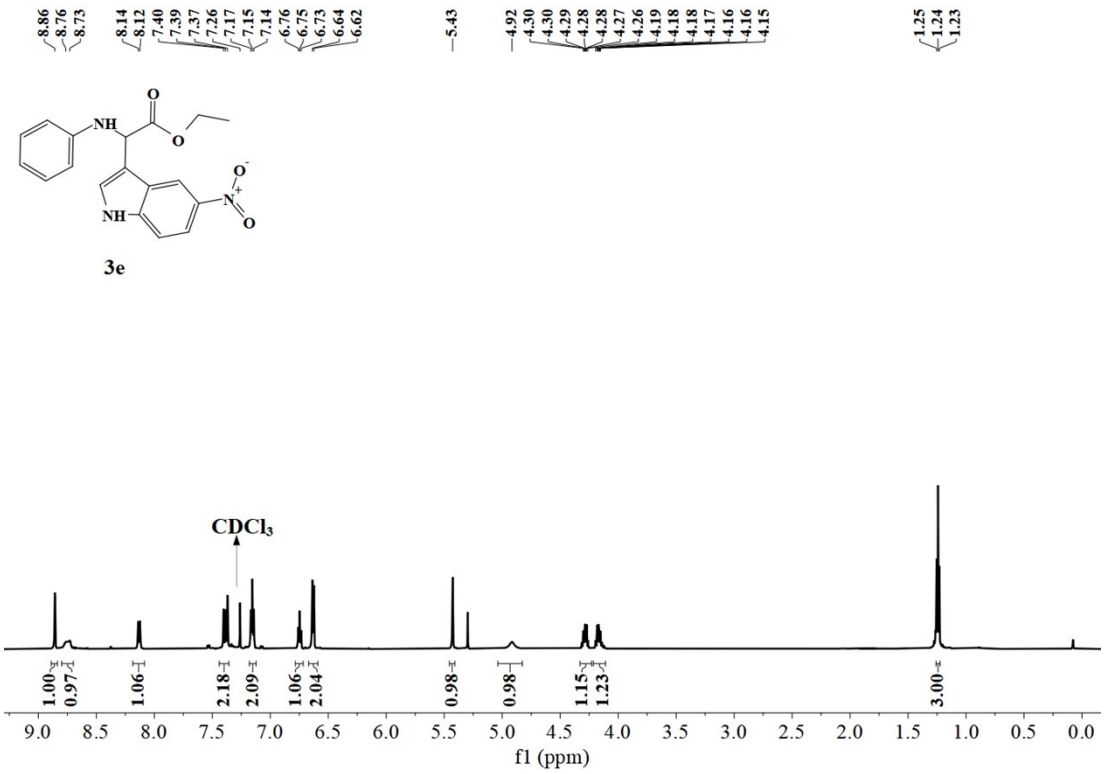


$^{1}$H NMR (600 MHz, $CDCl_3$) spectrum for **3e**

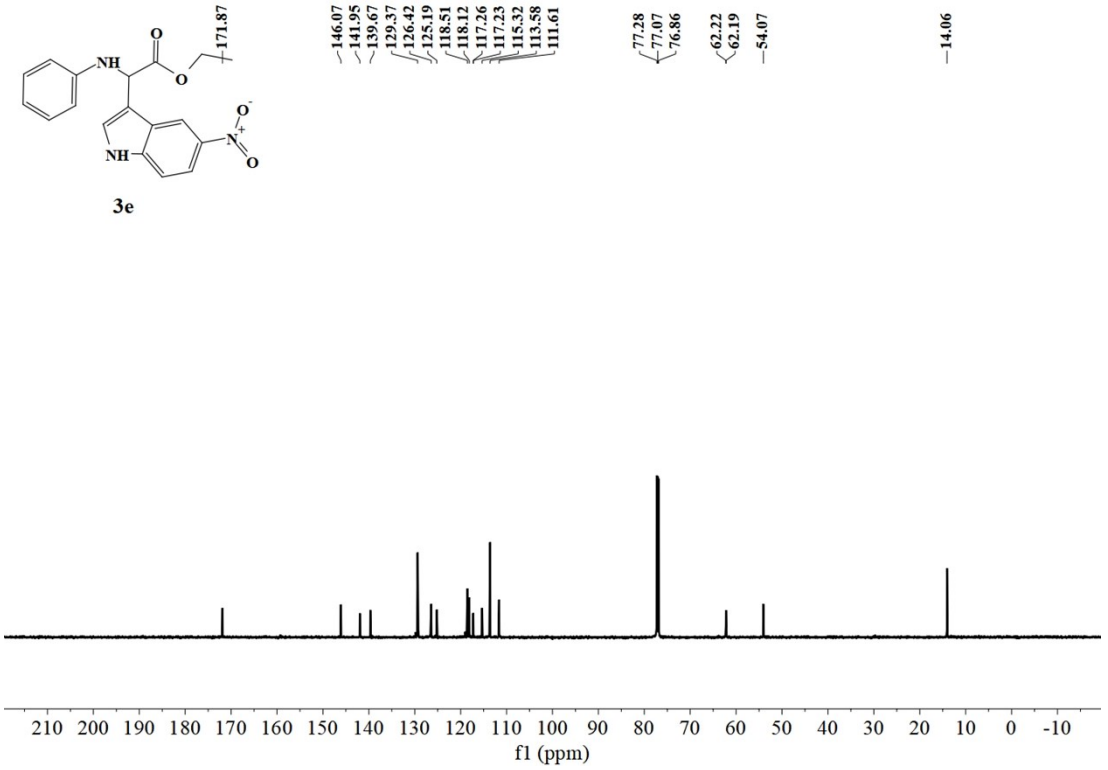


$^{13}$C NMR (151 MHz, $CDCl_3$) spectrum for **3e**

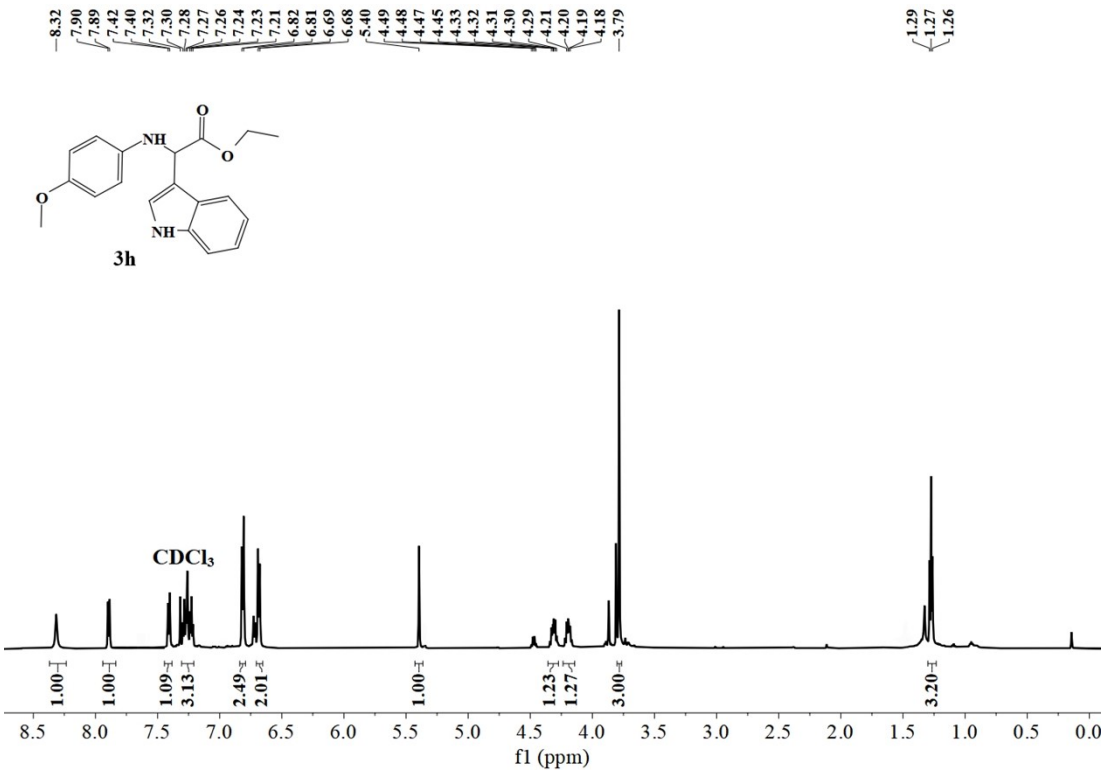


$^{1}$H NMR (600 MHz, $CDCl_3$) spectrum for **3h**

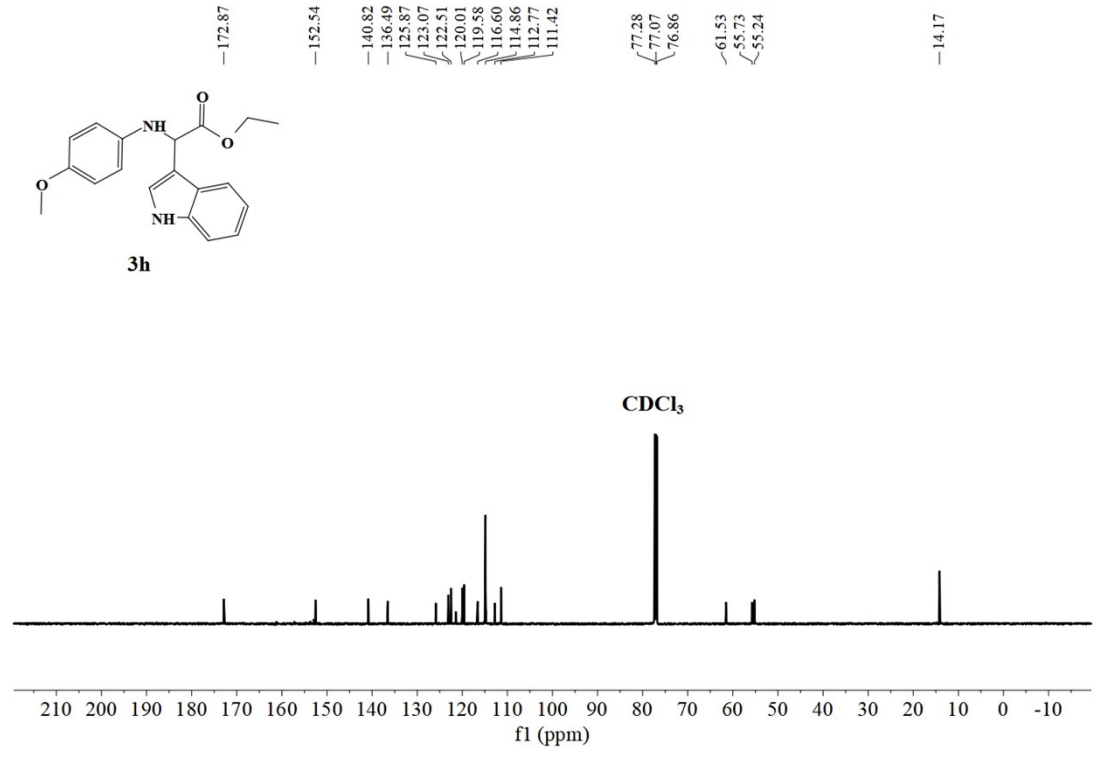


$^{13}$C NMR (151 MHz, $CDCl_3$) spectrum for **3h**

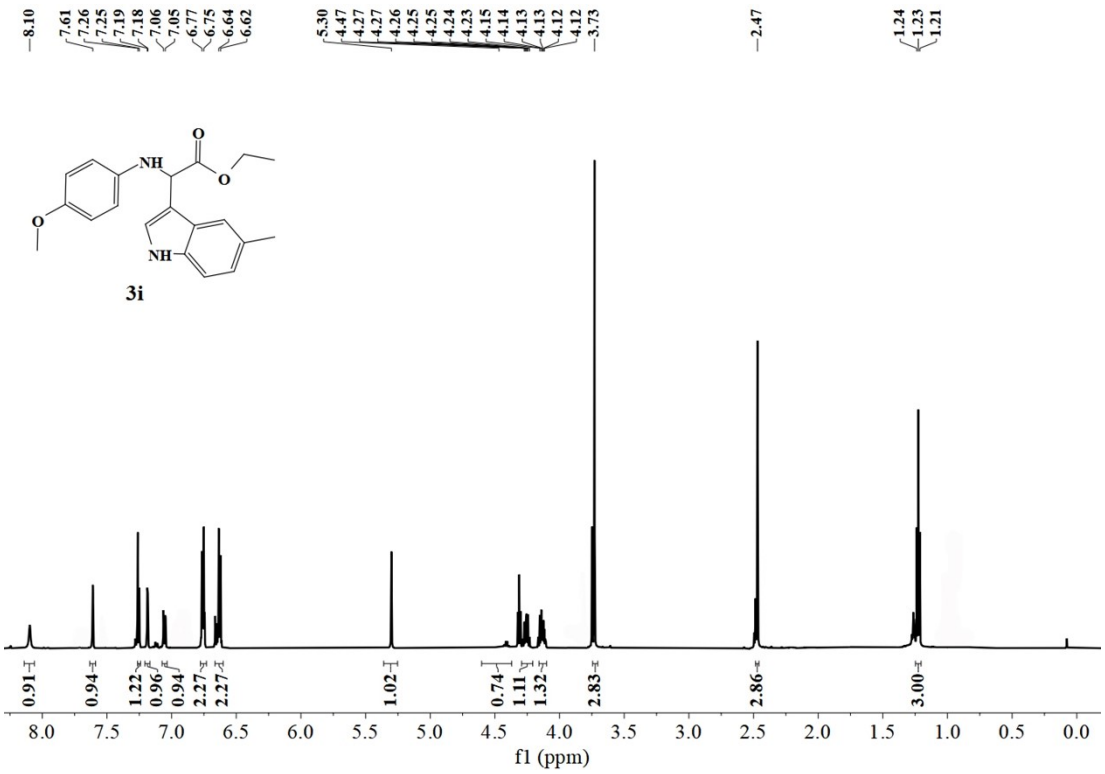


$^{1}$H NMR (600 MHz, $CDCl_3$) spectrum for **3i**

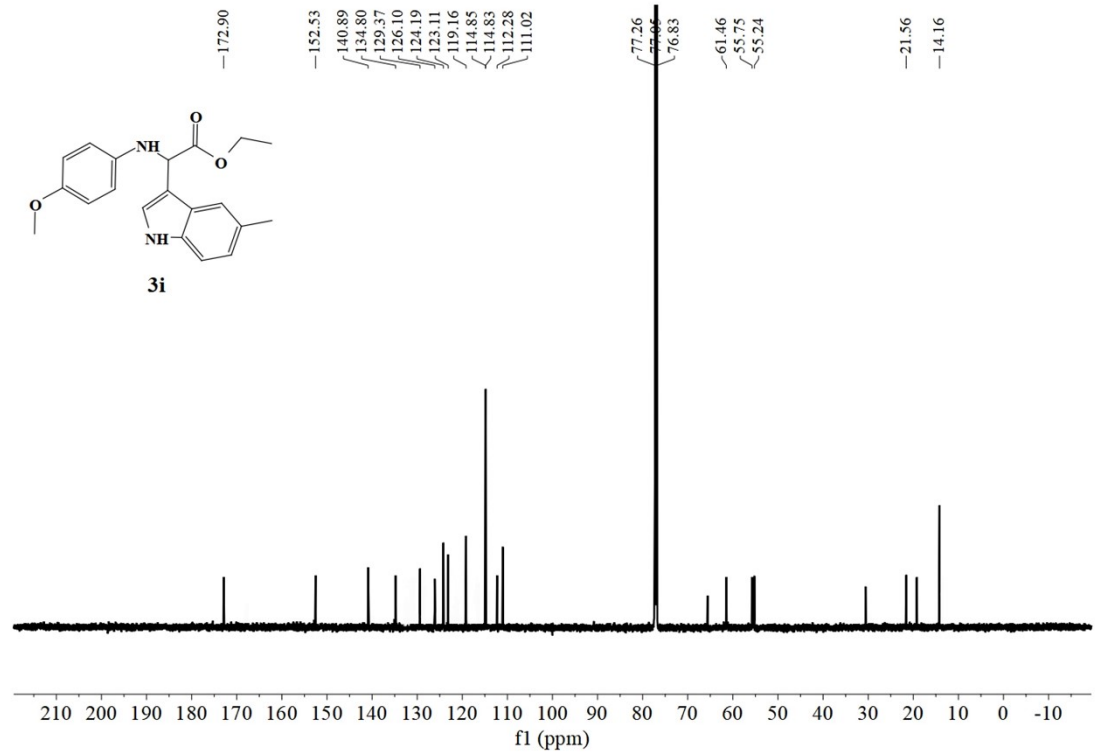


$^{13}$C NMR (151 MHz, $CDCl_3$) spectrum for **3i**

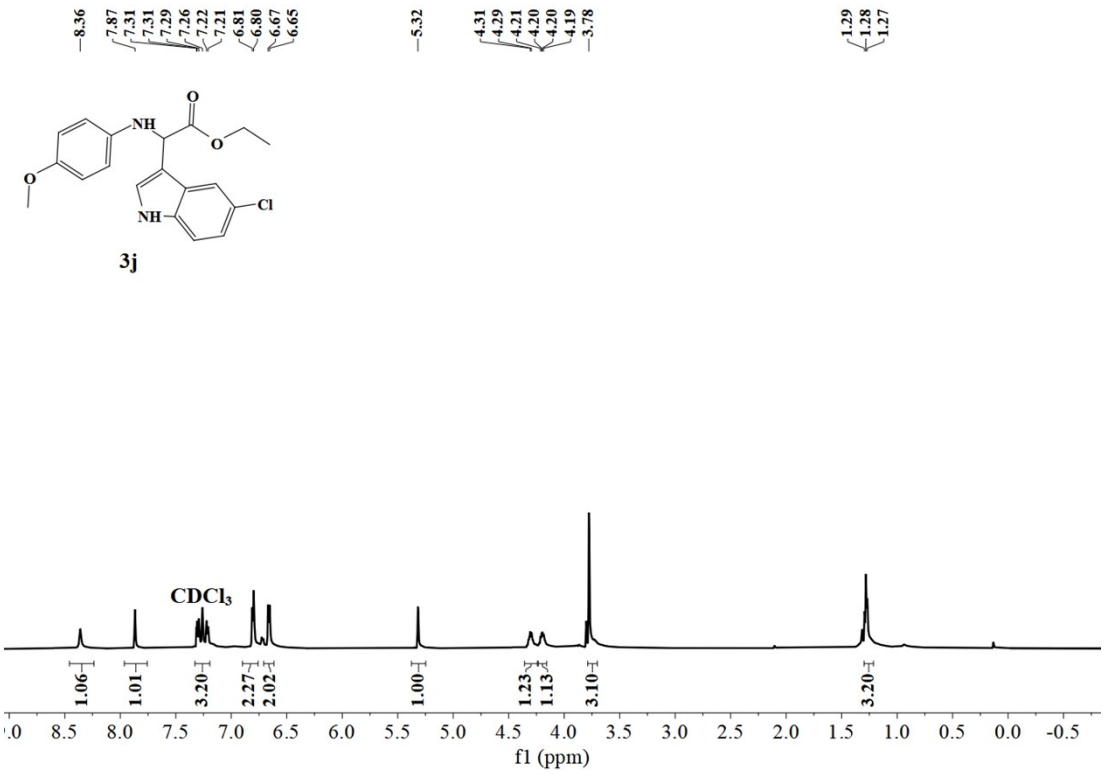


$^{1}$H NMR (600 MHz, $CDCl_3$) spectrum for **3j**

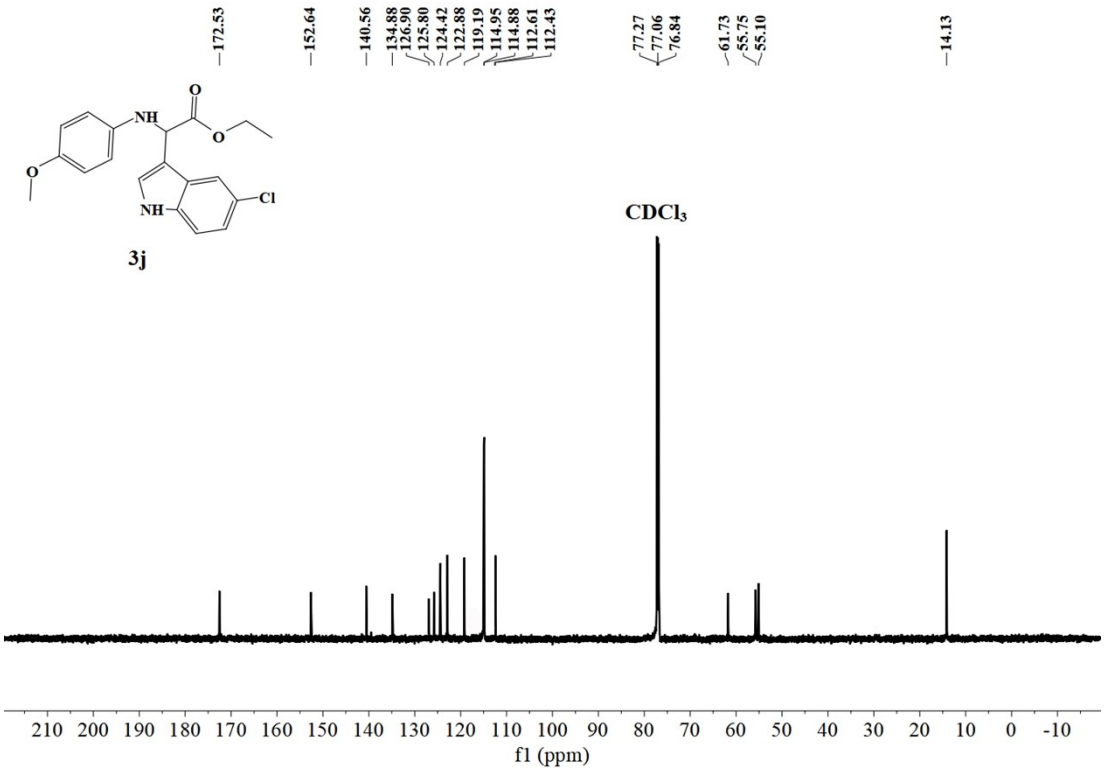


$^{13}$C NMR (151 MHz, $CDCl_3$) spectrum for **3j**

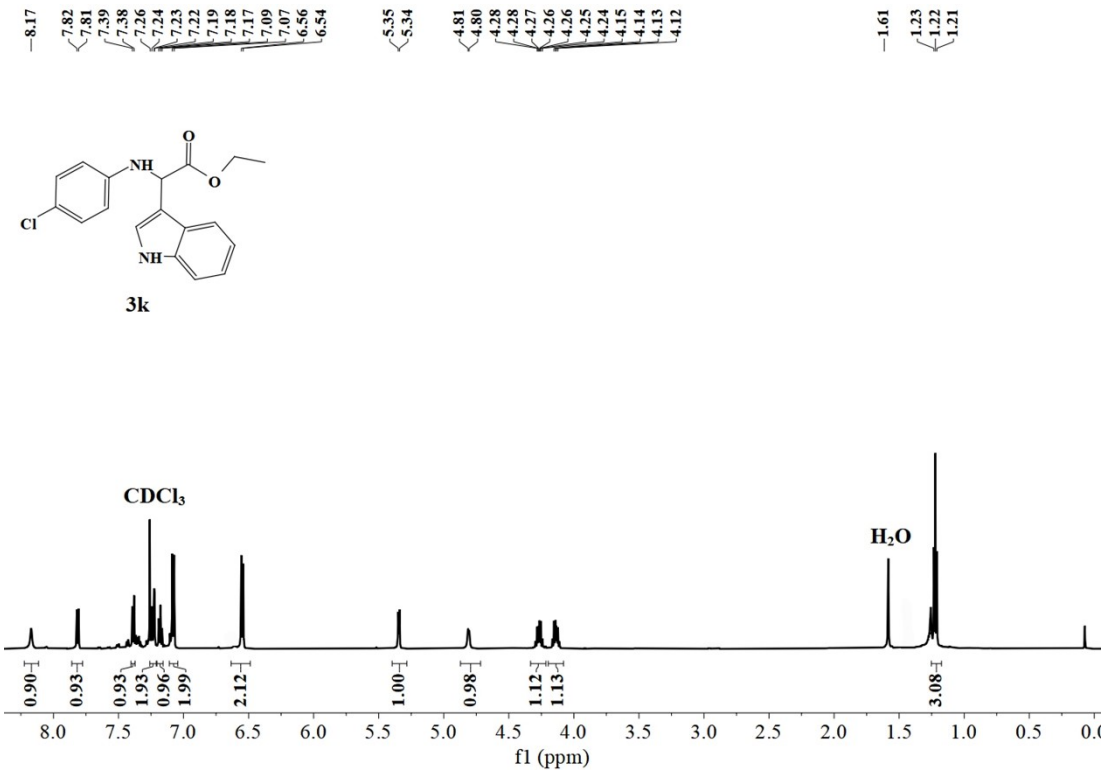


$^{1}$H NMR (600 MHz, $CDCl_3$) spectrum for **3k**

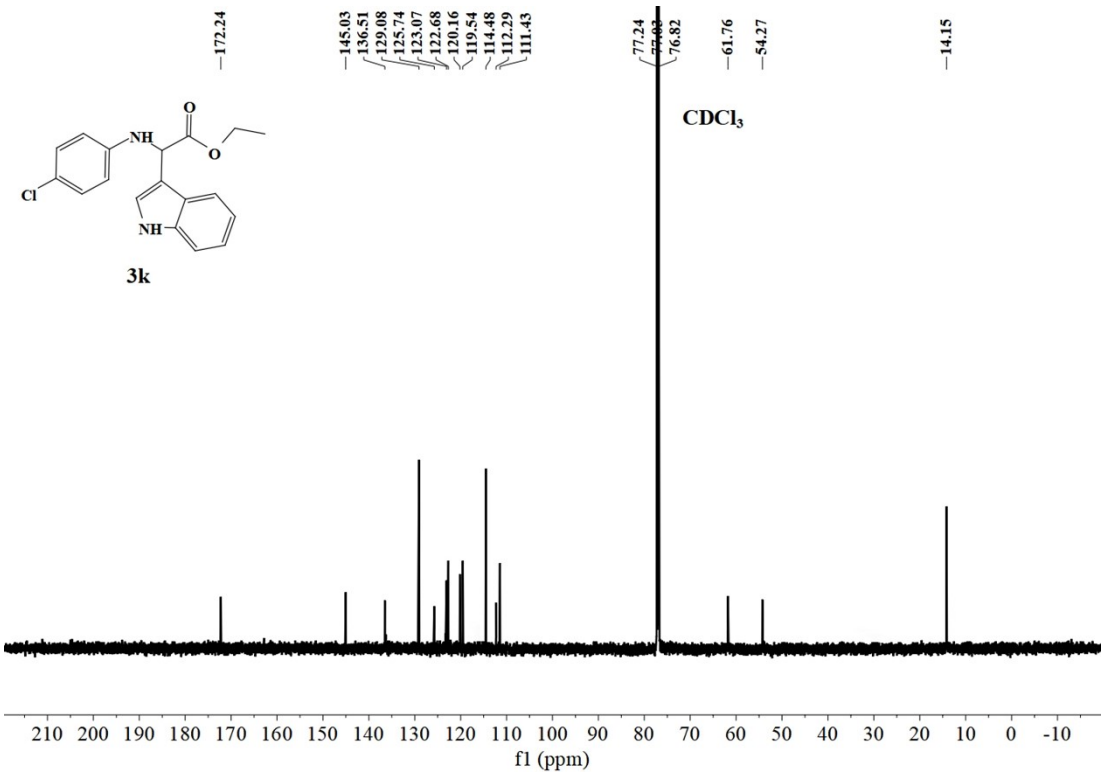


$^{13}$C NMR (151 MHz, $CDCl_3$) spectrum for **3k**

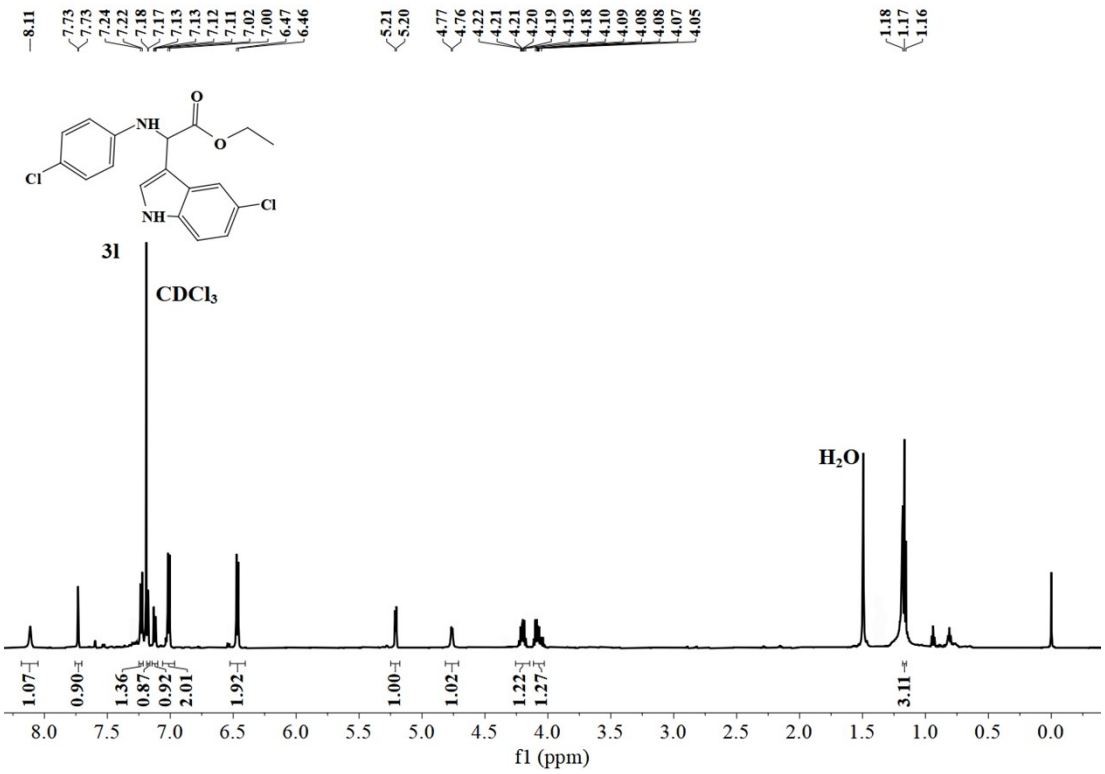


$^{1}$H NMR (600 MHz, $CDCl_3$) spectrum for **3l**

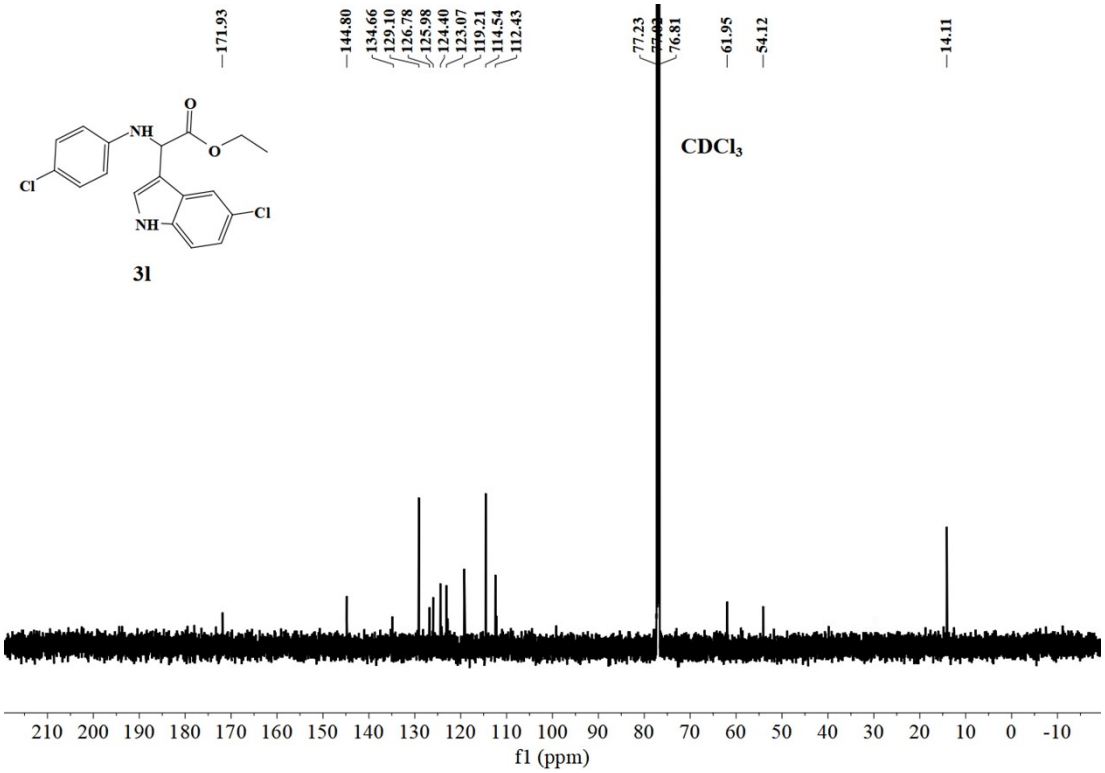


$^{13}$C NMR (151 MHz, $CDCl_3$) spectrum for **3l**

# Section S7. References


[1] Feng, D. W.; Gu, Z. Y.; Li, J.-R.; Jiang, H.-L.; Wei, Z.; Zhou, H.-C. Zirconium-Metalloporphyrin PCN-222: Mesoporous Metal-Organic Frameworks with Uultrahigh Stability as Biomimetic Catalysts. *Angew. Chem. Int. Ed.* **2012**, *51*,10307-10310;

[2] Zhang, L. J.; Yuan, J. C.; Ma, L. J.; Tang, Z. Y.; Zhang. X. M. Selective Hydroboration of Alkynes via Multisite Synergistic Catalysis by PCN-222(Cu). *J. Catal.* **2021**, *401*, 63-69;

[3] Yang, G.; Shi, W. W.; Qian, Y. Y.; Zheng, X.; Meng, Z.; Jiang, H.-L. Turning on Asymmetric Catalysis of a Chiral Metal-Organic Frameworks by Imparting Chiral Microenvironment. *Angew. Chem. Int. Ed*. **2023**, *62*, e202308089;

[4] Wang, L.-L.; Yang, C.-X.; Yan, X.-P. Exploring Fluorescent Covalent Organic Frameworks for Selective Sensing of $Fe^{3+}$. *Sci. China Chem.* **2018**, *61*, 1470-1474;

[5] Zhang, H.-Y.; Yang, Y.; Li, C.-C.; Tang, H.-L.; Zhang, F.-M.; Zhang, G.-L.; Yan, H. A New Strategy for Constructing Covalently Connected MOF@COF Core-Shell Heterostructures for Enhanced Photocatalytic Hydrogen Evolution. *J. Mater. Chem. A*, **2021**, *9*, 16743-16750;

[6] Li, Z. P.; Wang, J. A.; Ma, S.; Zhang, Z. W.; Zhi, Y. F.; Zhang, F. C.; Xia, H.; Henkelman, G.; Liu, X. M. 2D Covalent Organic Frameworks for Photosynthesis of *α*-trifluoromethylated Ketones from Aromatic Alkenes. *Appl. Catal. B: Environ.* **2022**, *310*, 121335-121345;

[7] Zhu, S.; Rueping, M. Merging Visible-Light Photoredox and Lewis Acid Catalysis for the Functionalization and Arylation of Glycine Derivatives and Peptides. *Chem. Commun.,* **2012**, *48*, 11960–11962.

[8] Huo,C.; Wang, C.; Wu, M. Jia, X. Xie, H.; Yuan, Y. Copper(I) Chloride-Catalyzed Aerobic Oxidative Arylation of Glycine Ester and Amide Derivatives. *Adv. Synth. Catal.* **2014,** *356*, 411 415.

[9] Zhang,Y.; Ni, M. Feng, B. Iron-catalyzed Direct α-arylation of α-amino Carbonyl Compounds with Indoles. *Org. Biomol. Chem.,* **2016,** *14*, 1550–1554.

[10] Kumar, G.; Pillai, R. S.; Khan, N. H.; Neogi, S. Structural Engineering in Pre-Functionalized, Imine-Based Covalent Organic Framework via Anchoring Active Ru(II)-Complex for Visible-Light Triggered and Aerobic Cross-Coupling of α-amino Esters with Indoles. *Appl. Catal. B: Environ.* **2021,** *292,* 120149.

[11] Wang, Z.-Q.; Hu, M.; Huang, X.-C.; Gong, L.-B.; Xie, Y.-X.; Li, J.-H. Direct α-arylation of α-amino Carbonyl Compounds with Indoles Using Visible Light Photoredox Catalysis. *J. Org. Chem.* **2012**, *77*, 8705-8711.

[12] Yang, X.; Li, L.; Li, Y. Zhang, Y. Visible-Light-Induced Photocatalytic Aerobic Oxidative $Csp^3$–H Functionalization of Glycine Derivatives: Synthesis of Substituted Quinolines. *J. Org. Chem.* **2016**, *81*, 12433–12442.